Evaluation of a Procedure for Encapsulation and Epoxy Injection of Corroding Reinforced Concrete Structures

by

Muhammed Alp Ünal, B.S.

Thesis

Presented to the Faculty of the Graduate School of

The University of Texas at Austin

in Partial Fulfillment

of the Requirements

for the Degree of

Master of Science in Engineering

The University of Texas at Austin

May 1998

Evaluation of a Procedure for Encapsulation and Epoxy Injection of Corroding Reinforced Concrete Structures

Approved by
Supervising Committee:

James O. Jirsa

David W. Fowler

Dedication

To my parents for their love and support

Acknowledgements

I would like to express my most sincere appreciation and gratitude to Dr. James O. Jirsa for supervising the research in which this thesis is based. The possibility of successfully completing this research would not have existed without his unconditional support.

Special thanks to Dr. Sharon L. Wood for encouraging me to attend The University of Texas at Austin and supporting me during my first semester.

Particular thanks to Dr. David W. Fowler and Harowel G. Wheat for their help and interest.

I would like to thank Hardcore DuPont Composites and Dow Chemical Company for sponsoring the project. Their funding provided means to complete this thesis. The interest and cooperation of Grant Corboy, Mac Puckett, and David Ridley were essential for the completion of the project. Also thanks to Texas Department of Transportation for providing the specimens used in the project.

A sincere recognition goes to Dr. Engin Karaesmen and Dr. Erhan Karaesmen of Middle East Technical University, Ankara, Turkey, for their help, advice, and support.

My sincere thanks are extended to the Ferguson Structural Engineering Laboratory staff who cooperated to make this project possible. Also special thanks to Enrique Vaca, Stewart Verhulst, and Laura Fuentes for their help during

various stages of the project. Timely completion of this project would not have been possible without their help.

Great gratitude is extended to Sergio Brena, Ahmet Yakut, Kevin Clinch, Craig Chamberlain, Jeff West, Blanca Velazquez, Brad Koester, and many other fellow graduate students for their friendship.

Finally, I would like to extend the deepest gratitude to my parents. They have always believed in me and supported me.

May 8, 1998

Abstract

Evaluation of a Procedure for Encapsulation and Epoxy Injection of Corroding Reinforced Concrete Structures

Muhammed Alp Ünal, M.S.E.

The University of Texas at Austin, 1998

Supervisor: James O. Jirsa

A procedure involving encapsulation and epoxy injection for extending the service life of corroding reinforced concrete structures was studied. Specimens that were exposed to a corrosive environment for four and a half years were used. Corrosion activity in the specimens was well-documented. The specimens repaired using the encapsulation procedure and companion unrepaired specimens were exposed to a corrosive environment for one year and were monitored. At the end of the study the specimens were opened to examine the condition of reinforcing bars and concrete inside the specimens.

Table of Contents

List of Tables

List of Figures

CHAPTER 1

INTRODUCTION

1.1 BACKGROUND

Corrosion of reinforcement in structural concrete is a major concern since it costs billions of dollars each year to repair and rehabilitate current construction. Construction costs protection against corrosion are significant. Corrosion damage can cause safety hazards.

Corrosion has always been of special concern for structures exposed directly or indirectly to sea water. When extensive use of salt on highways and bridges began in 1960s, tracking of chloride-containing deicing chemicals onto structures made with calcium chloride or other chloride-containing admixtures created similar corrosion problems in many location away from the sea [Gibson, 1987]. Parking structures are particularly vulnerable to corrosion due to the transportation of chemicals by vehicles. There are many other cases where corrosion in reinforced concrete structures may be produced by other actions; such as chemical exposure, pollution, and sulfate attack [Nene, 1985].

Repair and rehabilitation of corrosion damaged structures is becoming increasingly important because deterioration rate of existing structures increases with age. Therefore, research is being conducted in order to find new ways to

protect against corrosion and new methods to repair and rehabilitate corrosion damage in the most efficient way.

1.2 Repair And Rehabilitation Of Corrosion Damage

1.2.1 Conventional Methods [Pfeifer, 1985b]

Depending on the degree of corrosion damage, there are several different procedures to repair corrosion damage.

If corrosion-related distress has progressed to serious spalling, then repair procedures generally involve most of the following:

- Removing unsound concrete and exposing reinforcing steel,
- Cleaning concrete and steel by sandblasting,
- Restoring reinforcement by replacing corroded bars if there is a significant loss of steel area, and protecting reinforcement,
- Using one of several patching techniques to restore concrete, usually to the original level,
- Applying paint or other appropriate surface coating.

If no spalling has occurred, pressure injection of epoxy alone may provide suitable repair. This can be done not only in structural cracks but also in corroded areas where distress is in early stages. If the cracks are active, however, a flexible material such as an elastomeric joint sealant may be required.

1.2.2 Advantages and Disadvantages of Conventional Repair Materials

Selection of materials and procedures is one of the most important aspects of corrosion repair. An important aspect of selection of materials and procedures for corrosion repair is that repairs to one part of the structure might aggravate corrosion in other parts of the structure [Maurisin, 1985]. The advantages and disadvantages of materials for corrosion-damage are tabulated by Pfeifer [1985b] and given in Table 1.1. Even though this table is for corrosion-damaged vertical surfaces, it provides a very good summary of the conventional repair materials available.

1.2.3 New Techniques

With the increasing knowledge of corrosion and developments in new materials, many new techniques for repair of corrosion damage are either being used or being evaluated for future use. Use of fiber reinforced composite plates in combination with injection of resin or epoxies is being utilized

Encapsulation has proven to be useful for seismic repair and rehabilitation of structures. These techniques have been used for seismic upgrading of bridge piers for strength and ductility in California [Roberts, 1997].

Table 1.1. Repair Materials for Corrosion-Damaged Vertical Surfaces

Description of material or process	Advantages	Disadvantages	Comments
Shotcrete- a mixture of water, cement, and aggregate combined and sprayed or gunned at high velocity onto the surface to be restored.	Only limited forming needed; bond to properly prepared old concrete is usually excellent.	Rebound; a significant amount of material bounces away from the surface being shotcreted and is thereby lost.	Reinforcement of patch with welded wire fabric or small diameter wire mesh advised.
Hand-applied latex -or polymer- modified portland cement mortar. Several commercially prepared products available.	Low permeability to water; good bond to properly prepared old concrete. High durability, crack resistance, and tensile strength.	Relatively high cost. Not extensively tested in vertical repairs.	Forming not required. Applied with trowel or spatula.
Low water-cement ratio concrete with entrained air and appropriate admixtures to produce a dense workable mix.	Lower cost for repair material, of particular importance for large repairs.	Forms are necessary, and may be difficult to support in some installations.	Water reducing admixtures suggested; superplasticizers may be appropriate. Check for compatibility with air entraining admixture.
Polymer concrete and mortars such as methyl methacrylate and epoxy concretes.	High strength, high durability, and good bond to properly prepared concrete.	Relatively expensive; forms needed for deep repairs, Some are flammable and toxic.	Detailed attention to manufacturer's recommendations required. Careful formulation needed to avoid problems due to differences of physical properties from those of adjoining concrete.
Epoxy injection-crack surface sealed except for injection ports inserted at intervals along crack. Epoxy is then pumped through ports. Proprietary pressurized systems available.	Very little surface preparation needed; strong bond and durability of patch.	Scar marks may be left on surface where crack was injected. Limited to areas where concrete had not yet spalled.	Structural quality bond is established but if large structural movements still occurring, new cracks may open.

1.3 THE CORROSION PROCESS

1.3.1 Definition [Fontana, 1986; Speller, 1952]

Corrosion is the deterioration or destruction of a metal by direct chemical or electrochemical reaction with its environment.

1.3.2 Corrosion Process of Reinforcing Steel in Concrete

Corrosion of reinforcement steel in concrete is a well understood process that involves the steel, oxygen, and an electrode. Especially in the regions of high humidity, or on highway bridges subjected to freeze-thaw cycles treated with sodium chloride, the presence of chloride in concrete turns it into an electrolyte. This results in galvanic currents that destroy the passivity or the protective film that protects the steel bar embedded in concrete and converts a small portion of the bar into an anode and a larger part of it into a cathode [Fontana, 1986; Gallegos, 1987].

The single bar corrosion process (Figure 1.1) involves metal dissolution at the anode and oxygen reduction or hydrogen gas evolution along the cathode depending upon the corrosive environment [5]. These reactions are given by Equations 1.1 through 1.3. The corrosion of reinforcing steel is an electrochemical process in which the chemical processes are accompanied by a flow of electricity. Corrosion leads to the formation of extremely unstable ferric oxide (Equation 1.4), which in the presence of oxygen, produces a corrosion product (rust) through a secondary chemical process (Equation 1.5) that occupies a much greater volume than the reinforcing steel. As a result, strong internal forces are developed and may cause concrete cracks to form parallel to the bar.

Carbon dioxide is available at the crack and carbonation occurs deeper into the concrete thereby speeding up the process. Loss of reinforcing steel area in concrete through corrosion may result in long-term structural disintegration and failures [Gallegos, 1987].

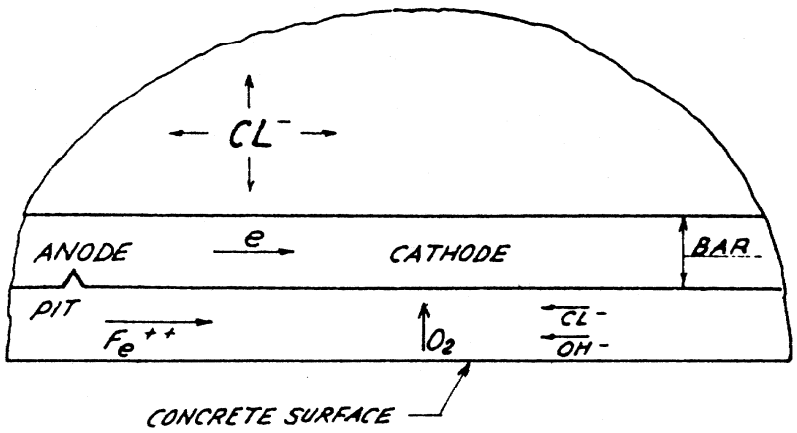

Figure 1.1 Single Bar Corrosion Process

Anodic Reaction:

$Fe + 2e^- \rightarrow Fe^{+2}$ Metal Dissolution (Equation 1.1)

Cathodic Reaction:

$2H_2O + O_2 + 4e^- \rightarrow 4OH^-$ Reduction of Oxygen (Equation 1.2)

or $2H^+ + 2e^- \rightarrow H_2$ Hydrogen Gas Evolution (Equation 1.3)

$$2Fe + 2H_2O + O_2 \rightarrow 2Fe(OH)_2$$ Formation of ferric oxide (Equation 1.4)

$$2Fe(OH)_2 \xrightarrow{O_2, H_2O} 2Fe(OH)_3$$ Formation of rust (Equation 1.5)

1.3.3 Factors Contributing to Corrosion Damage

Pfeifer [1985a] discusses the factors contributing to corrosion damage as:

- Age of the structure,
- Orientation of the concrete, i.e., the severity of environment in different faces of the structure due to wind, rain, etc.,
- Corrosive environment,
- Insufficient concrete cover for steel,
- Presence of dissimilar electrically conductive metals, i.e., galvanic coupling,
- Significant amounts of soluble chloride ion in concrete,
- Permeability of concrete cover,
- Failure of previous repairs.

1.4 OBJECTIVE OF THIS STUDY

The main objective of this study is to evaluate encapsulation and epoxy injection of corrosion damaged reinforced concrete structures to extend their service life. The encapsulation and epoxy injection procedure evaluated in this study was provided by Hardcore DuPont Composites.

The encapsulation and epoxy injection methods are used widely in seismic zones for upgrading strength and ductility but the durability aspects of the procedure have not been studied in any depth. The findings of this study are expected to aid in the repair of corrosion damaged reinforced concrete structures and to provide guidelines for using encapsulation and epoxy injection techniques for corrosion protection.

1.5 SCOPE

Six beams and five macro-cells that were exposed to a corrosive environment for four and a half years with well-documented corrosion data were used in this project. Specimens repaired using encapsulation and epoxy injection were compared with control specimens with no repair. All specimens were exposed to a corrosive environment of 3.5% by weight saline solution for one year. The same saline solution was used for the previous exposure and provides accelerated corrosion activity. Specimens were exposed to the saline solution as follows: 3 weeks dry, 1 week wet for the beams, and 2 weeks dry, 2 weeks wet for the macro-cells.

CHAPTER 2

HISTORY OF BEAMS AND MACRO-CELLS

2.1 GENERAL

Beams and macro-cells used for evaluating encapsulation and epoxy injection of corrosion damaged reinforced concrete structures for corrosion durability were cast 6 years ago by Kahhaleh [1994] as a part of a study to evaluate the corrosion performance of epoxy-coated reinforcement. 6 of the 34 beams and 5 of the 68 macro-cells were selected for this study.

2.2 BEAMS

2.2.1 Properties

The reinforced concrete beams were designed to simulate cracked, loaded concrete components exposed to high corrosive environments for the assessment of the durability of epoxy-coated bars in concrete. The beams are 200mm. (8in.) by 300mm. (12in.) in cross-section and 2.9m. (9ft.) long. There are two 10mm. (#3) black (uncoated) bars at the top and two 19mm. (#6) epoxy coated bars at the bottom. Also there is a 10mm. epoxy coated stirrup in the middle of the beams. A detail of the cross-section is shown in Figure 2.1.

The beams have different properties in order determine the effect of different parameters on the corrosion performance of epoxy-coated reinforcement.

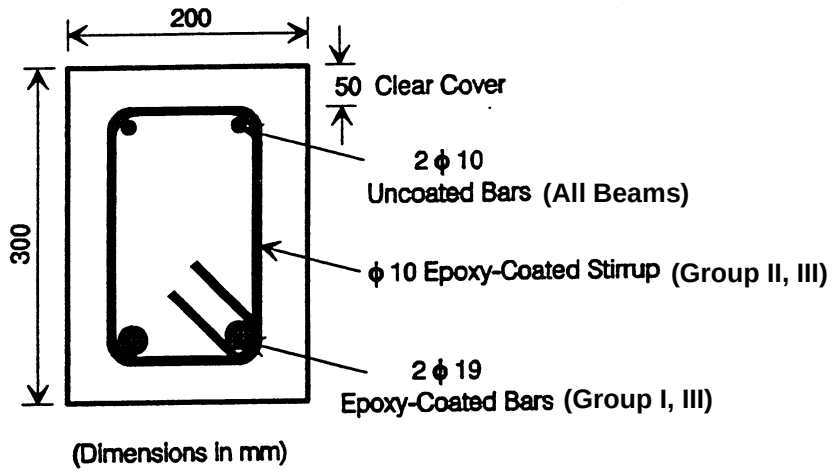

Figure 2.1. Cross-Section of the Beams and Bars Exposed.

In the previous test program, 3 groups of beams (I, II, and III) were studied. Details of group I, II, and III beams are shown in Figure 2.2, Figure 2.3, and Figure 2.4 respectively. A high permeability concrete was used in order to allow chlorides to penetrate into the concrete easily. The compressive strength-time curves for each group are shown in Figure 2.5. In addition to differences between groups, there are differences for beams within a group. In some beams the epoxy-coated reinforcement was damaged intentionally and left in a damaged condition while it was patched in other beams. In a few beams the bars were used as received. In some beams load was left on the beams to keep cracks open. Table 2.1 summarizes the properties for all 6 beams used in the encapsulation and

epoxy injection study. A description of the previous loading history and the loading history in this study is also provided in this table.

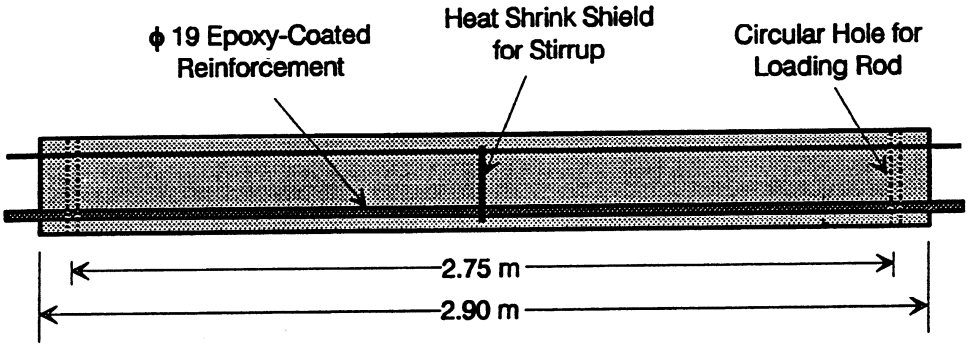

Figure 2.2. Details of Group I Beam Specimen (Longitudinal Steel).

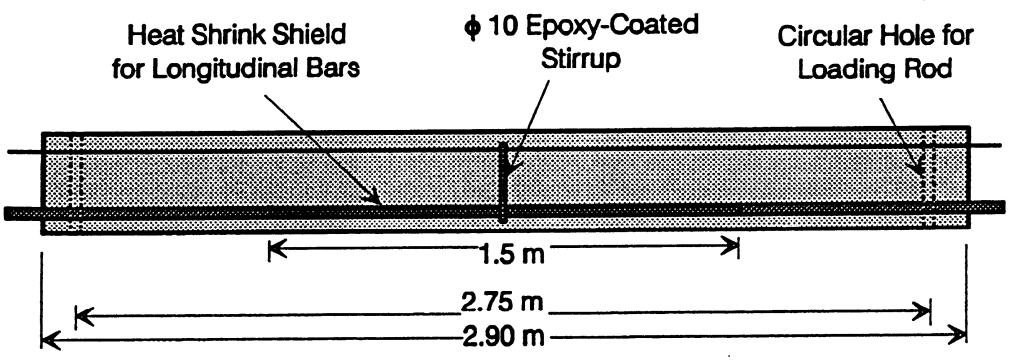

Figure 2.3. Details of Group II Beam Specimen (Stirrup).

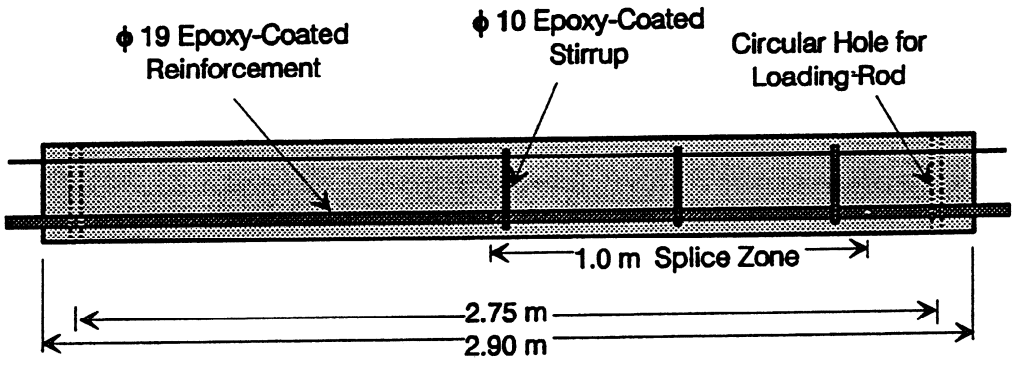

Figure 2.4. Details of Group III Beam Specimen (All Bars).

Table 2.1. Summary of Properties of Beams.

BEAM	GROUP/ PROPERTIES	BAR CONDITION (Damage Level and Condition)	LOADING HISTORY Previous Study	This Study	TYPE
B3	Group I Monitoring Longitudinal Bars (Stirrups were Covered)	As Received	Cracked, Unloaded	Cracked, Unloaded	Encapsulated
B6	Group I Monitoring Longitudinal Bars (Stirrups were Covered)	As Received	Cracked, Loaded	Cracked, Loaded	Encapsulated
B12	Group I Monitoring Longitudinal Bars (Stirrups were Covered)	3% Damaged	Cracked, Loaded	Cracked, Loaded	Control
B19	Group II Monitoring Stirrups (Longitudinal Bars were Covered)	As Received	Cracked, Loaded	Cracked, Unloaded	Encapsulated
B30	Group III Monitoring Longitudinal Bars and One Stirrup	Both Longitudinal Bars and Stirrups were 3% Damaged and Patched	Cracked, Unloaded	Cracked, Loaded	Control
B34	Group III Monitoring Longitudinal Spliced Bars and Three Stirrups	Stirrup 3% Damaged, Stirrup and Splice Bar End Patched	Cracked, Loaded	Cracked, Loaded	Encapsulated

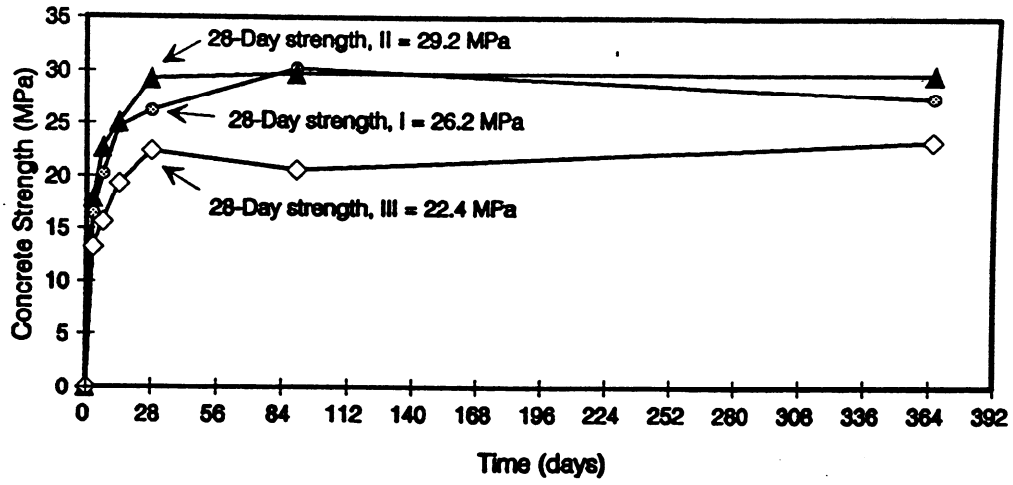

Figure 2.5. Compressive Strength-Time Curve of Concrete for Beam Groups.

2.2.2 Test Setup

Since the beams were designed for assessment of the durability of epoxy-coated bars in concrete under conditions simulating loaded structural elements, two replicates were available for each test condition to load the beams back to back as shown in Figure 2.6. Figures 2.7 and 2.8 show the beams under test and during loading.

In the previous study, the beams were subjected to a cyclic wet-dry exposure of 3.5% NaCl solution flowing over the beam surfaces within a defined exposure area (area of exposure was controlled using dikes, see dark area in Figure 2.6) for 3 days followed by a dry period of 11 days. Periodic wetting and drying was imposed to ensure continuous transport of corrosive substances to steel surfaces to promote corrosion. The cracked beams were subjected to loading

and unloading cycles twice during each exposure cycle: one time during wetting and the other during drying. Five load cycles were imposed each time up to a level producing the selected maximum crack width.

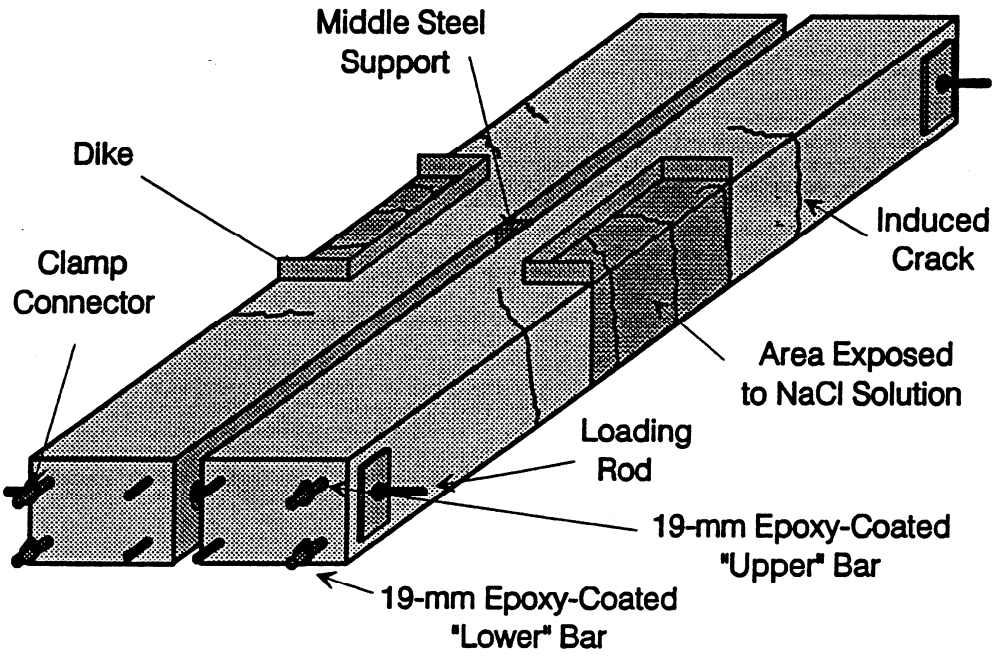

Figure 2.6. Model of Beam Exposure Test Specimens.

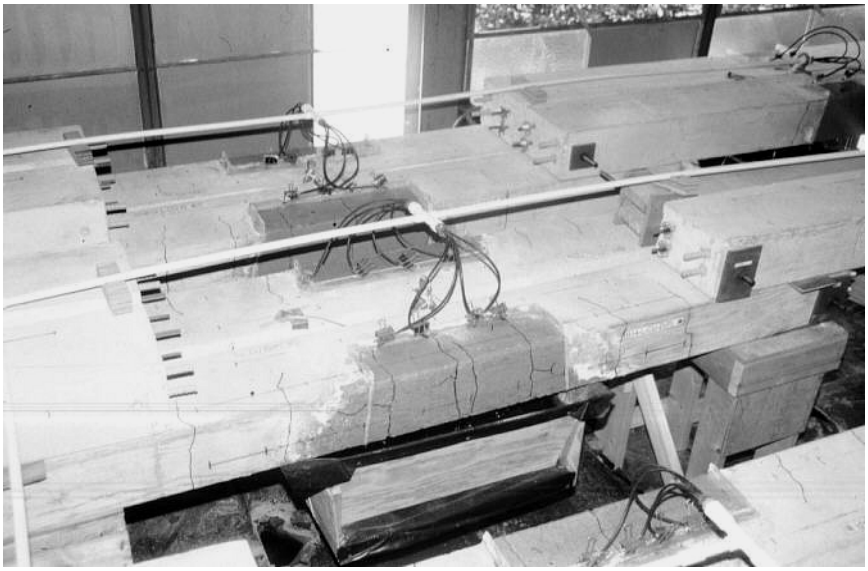

Figure 2.7. Beam Exposure Test Setup.

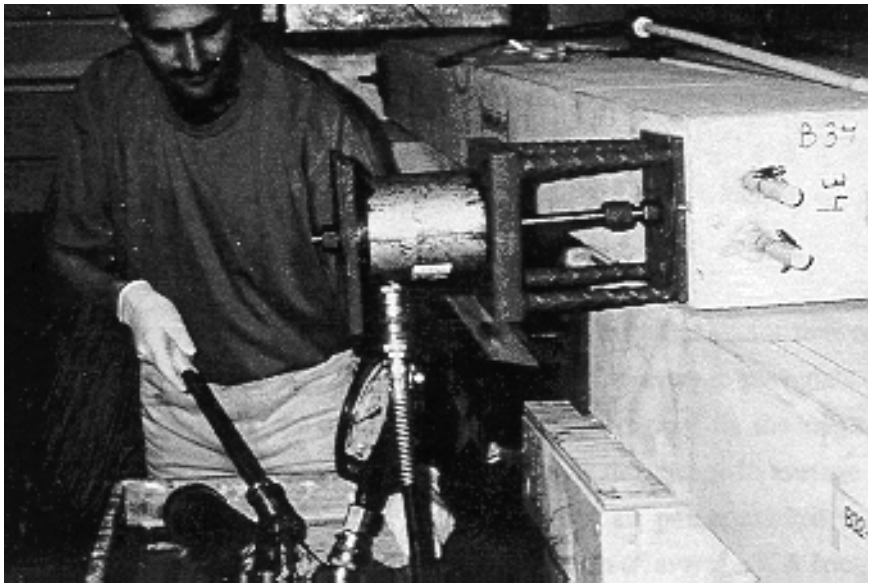

Figure 2.8. Loading Process.

2.2.3 Monitoring

The beams were monitored by taking half-cell potential readings according to ASTM C876-87 [1987] throughout the four and a half years duration of the project. The schematic of the half-cell potential measurement circuit is shown in Figure 2.9. The readings for longitudinal bars and stirrups inside the concrete were taken periodically against a saturated calomel reference electrode (SCE). The readings were taken along the bars every 6in. for longitudinal reinforcement and 2 to 4in. for the stirrups in order to detect any localized corrosion in the bars. Points of half-cell potential measurements are shown in Figure 2.10.

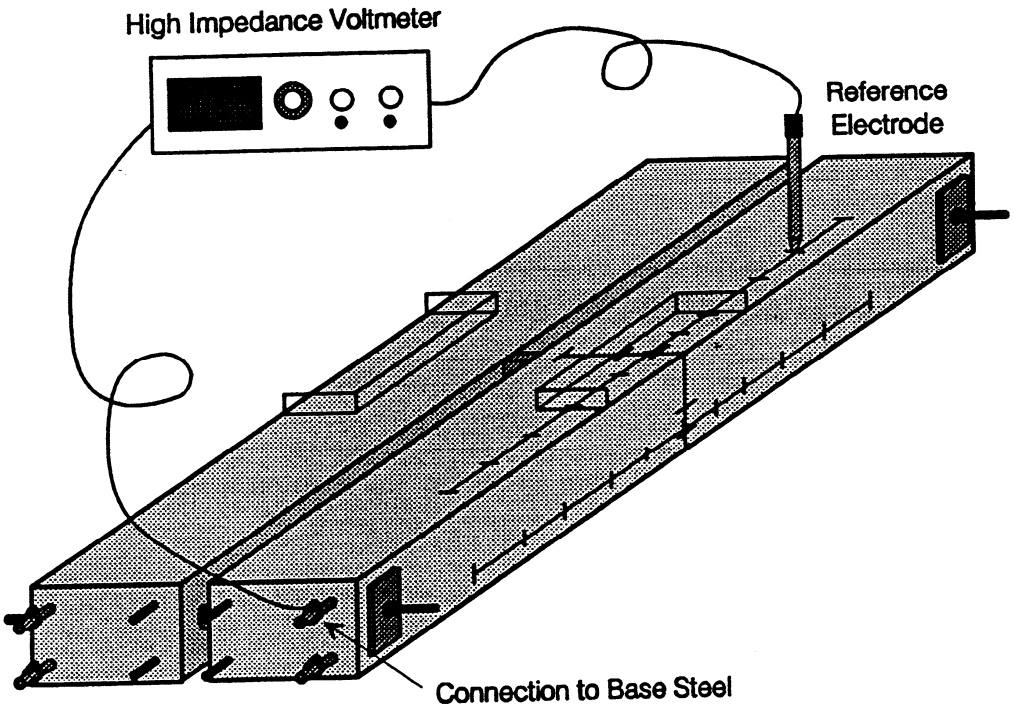

Figure 2.9. Schematic Diagram of Half-Cell Measuring Circuit.

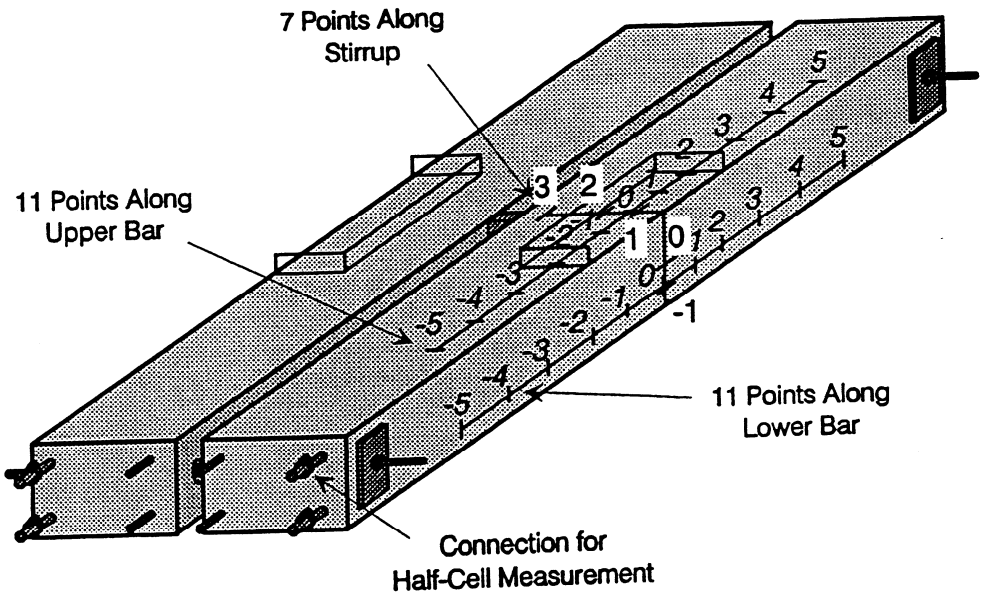

Figure 2.10. Points of Half-Cell Measurement.

2.2.4 Half-Cell Potentials

The half-cell potential readings (mV. vs. SCE) versus the time of exposure throughout the duration of the previous study are shown in Figures 2.11 through 2.16. In the graphs, black bar is the uncoated bar, epoxy 1 is the "upper" epoxy-coated bar when the beams are in exposure position (on their side), and epoxy 2 is the "lower" epoxy-coated bar in the exposure position (Figure 2.6). Monitoring of the black bars began well into the study.

According to ASTM C876-87 [1987] "half-cell potentials demonstrate the thermodynamic behavior of reinforcing steel in concrete". The probability of

corrosion of uncoated steel in concrete is determined by the empirical half-cell potential criteria shown in Table 2.2.

Table 2.2. Interpretation of Half-Cell Potentials Based on ASTM C876-87.

	Half-Cell Potential Reference	
Probability of Corrosion	**Copper/Copper Sulfate, CSE (mV)**	**Saturated Calomel, SCE (mV)**
Less than 10% if potential is less negative than	-200	-125
More than 90% if potential is more negative than	-350	-275
Uncertain if potential is between	-200 and -350	-125 and -275

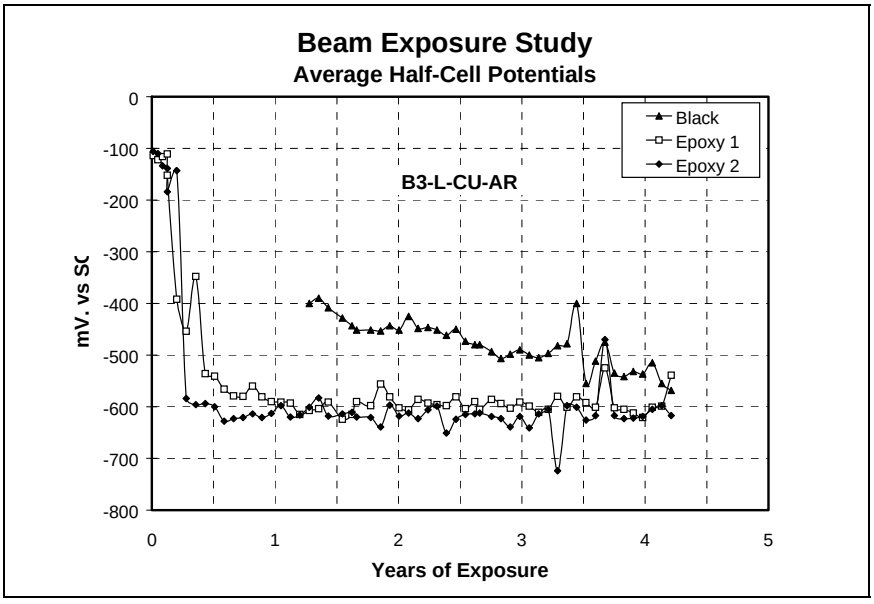

Figure 2.11. Half-Cell Potential Readings for Beam 3.

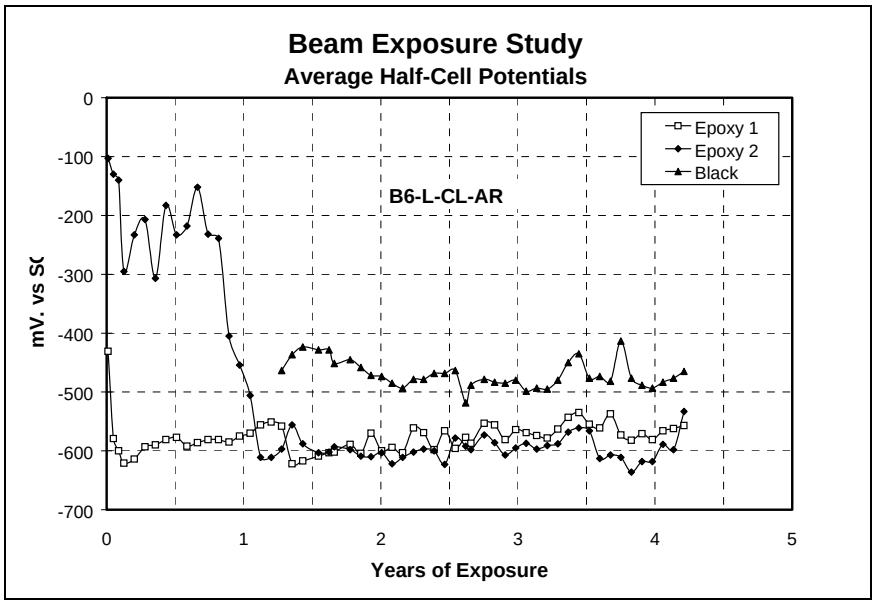

Figure 2.12. Half-Cell Potential Readings for Beam 6.

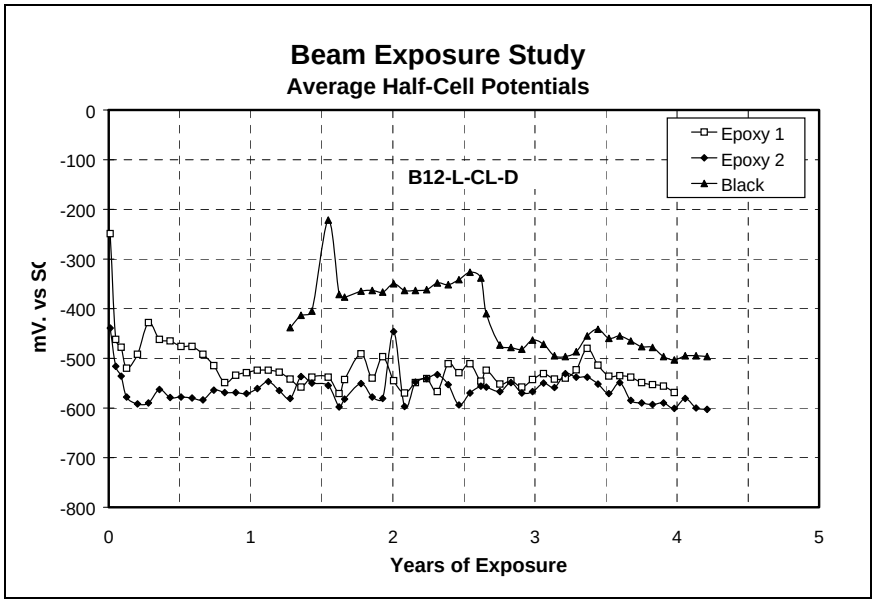

Figure 2.13. Half-Cell Potential Readings for Beam 12.

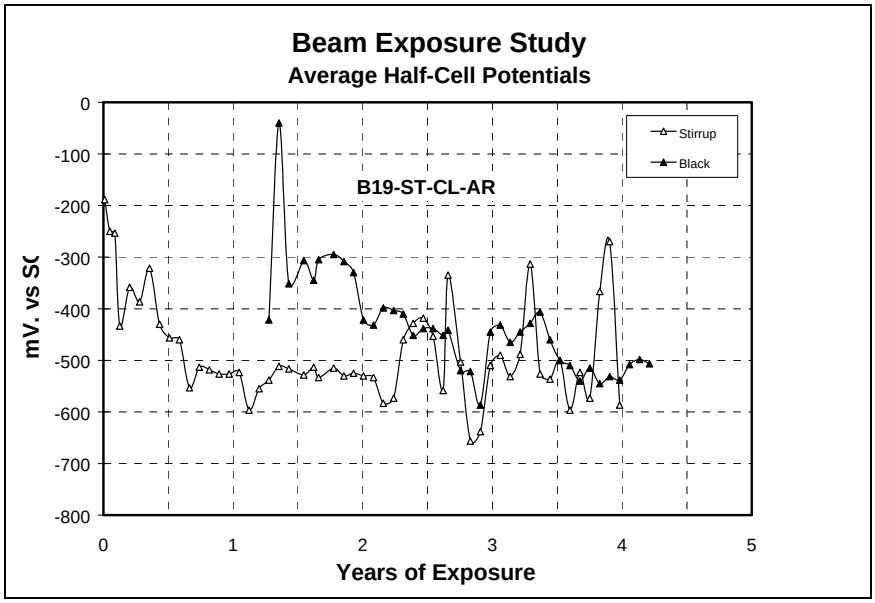

Figure 2.14. Half-Cell Potential Readings for Beam 19.

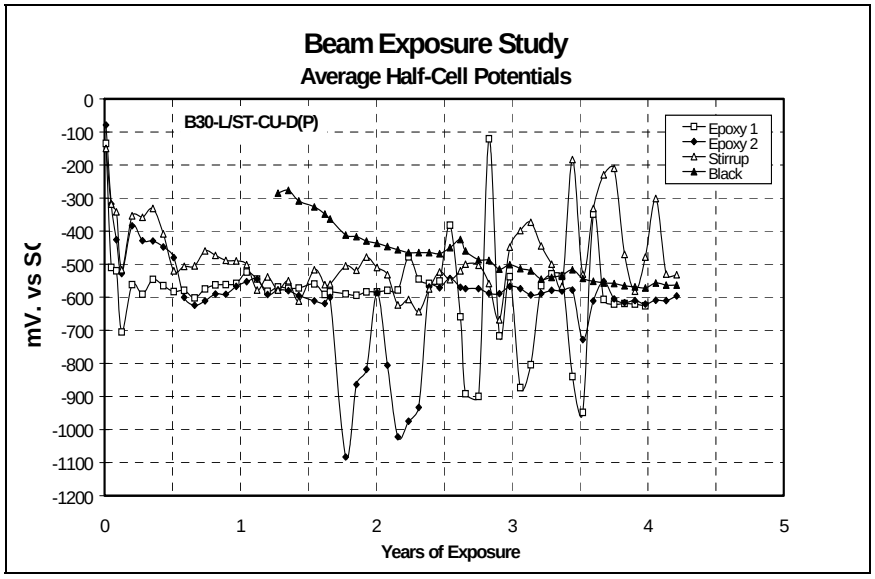

Figure 2.15. Half-Cell Potential Readings for Beam 30.

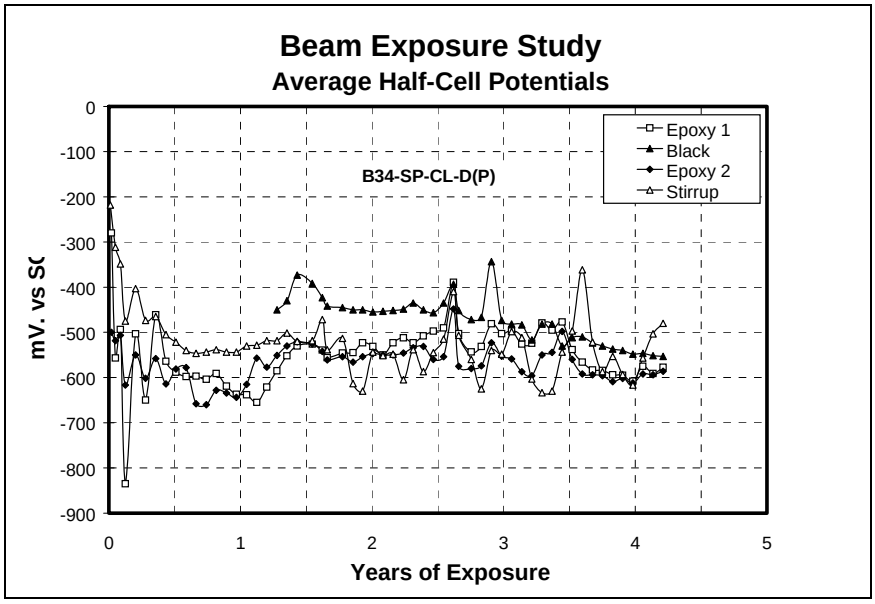

Figure 2.16. Half-Cell Potential Readings for Beam 34.

2.2.5 Chloride Contents

In addition to half-cell potential measurements, the chloride content was measured at the end of the study. The readings ranged from 0.46% to 1.07% [Vaca, 1998] and they are discussed in detail in Chapter 5.

2.3 MACRO-CELLS

2.3.1 Properties

The macro-cells are concrete prisms that were designed to simulate the conditions of a bridge deck slab exposed to deicing salt. They are 148mm. (6in.) by 300mm. (12in.) in cross-section and 225mm. (9in.) long. They have a bent, epoxy-coated 25mm. bar at the top and three straight, 28mm. bars at the bottom. Cross-sections of macro-cell specimens are shown in Figure 2.17.

There were several different groups of macro-cells where different parameters such as deformation pattern of ribs, epoxy-coating damage levels, and damage conditions were considered. Types of macro-cell specimens used for the encapsulation program were all B Series macro-cells which have cross ribs while the A Series macro-cells had parallel ribs. The summary of damage to bars in the Series B macro-cells used in the encapsulation study are given in Table 2.4.

Table 2.4. Summary of Macro-Cell Bar Damage.

Specimen - Type	Epoxy Coating Damage Level		Damage Condition	
	Spots > 6x6mm	Pinholes < 1%	Patched	Not Patched
1B8 - Encapsulated	Control Specimen - Uncoated Bars			
1B* - Encapsulated	Additional Specimen - Very Thin Coating			
3B9 - Control	●		●	
2B10 - Encapsulated	●			●
2B11 - Control		●		●

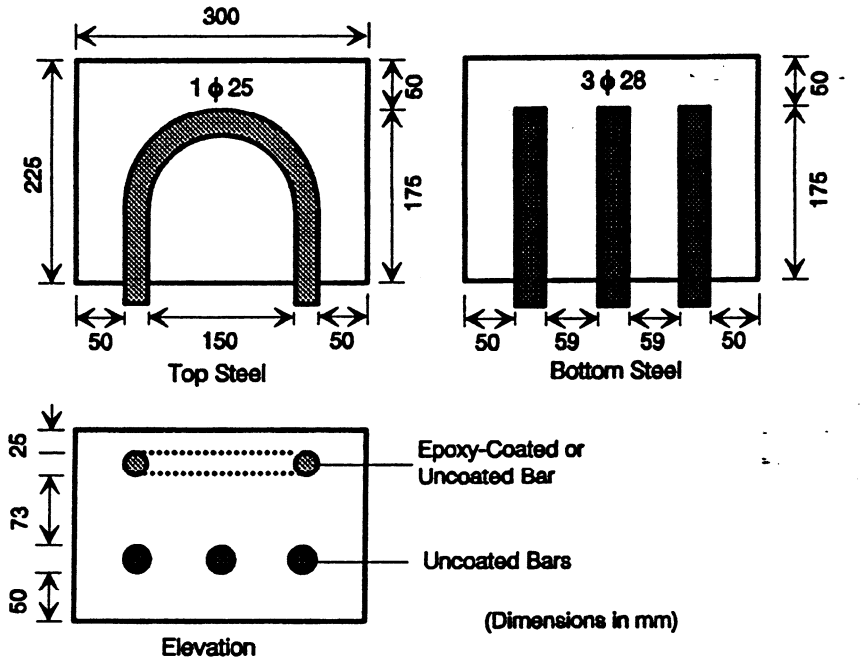

Figure 2.17. Details of Series B Macro-Cell Specimen.

All macro-cells had the same concrete properties. The compressive strength-time curve is shown in Figure 2.18.

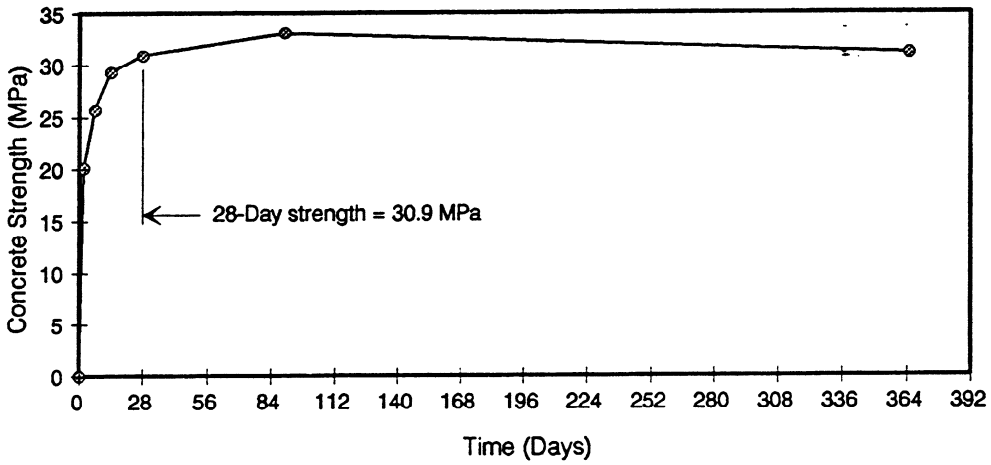

Figure 2.18. Compressive Strength-Time Curve for Macro-Cell Concrete.

2.3.2. Test Setup

Since the macro-cells were designed to simulate the conditions of a bridge deck exposed to salt solution, the conditions were intended to be as close as possible to bridge deck exposure. To do this; a 3.5% NaCl solution was ponded on the top surfaces for two weeks followed by a two week dry period. The solution was removed during the dry period. Plexiglass dikes 75mm. (3in.) high were mounted with silicon to contain the salt solution. A schematic of the specimens is shown in Figure 2.19. The specimens were placed on shelves on narrow wooden strips to allow air circulation under the soffits. Plywood was placed on top of the dikes in order to prevent evaporation.

2.3.3 Monitoring

Top and bottom reinforcing layers were linked using a 100ohm resistor. The voltage drop across this resistor was measured periodically and the voltage was converted to current using Ohm's Law. Due to the large number of specimens in the previous study, it was found more suitable to hook up all the specimens to a data acquisition system to measure the macro-cell current.

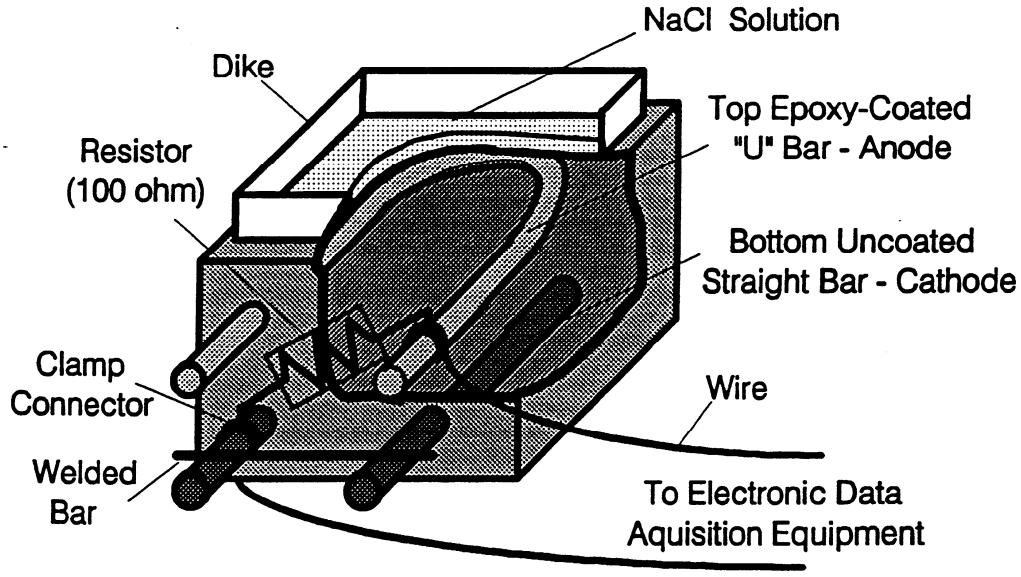

Figure 2.19. Macro-Cell Specimen Schematic.

2.3.4 Corrosion Currents

The current obtained by converting the macro-cell potential readings using Ohm's Law versus the time of exposure throughout the duration of the previous study are shown in Figure 2.20 through 2.24.

2.3.5 Chloride Contents

Chloride contents were measured at the end of the study. The readings ranged from 0.20% to 0.38% [Vaca, 1998] and they are discussed in detail in Chapter 5.

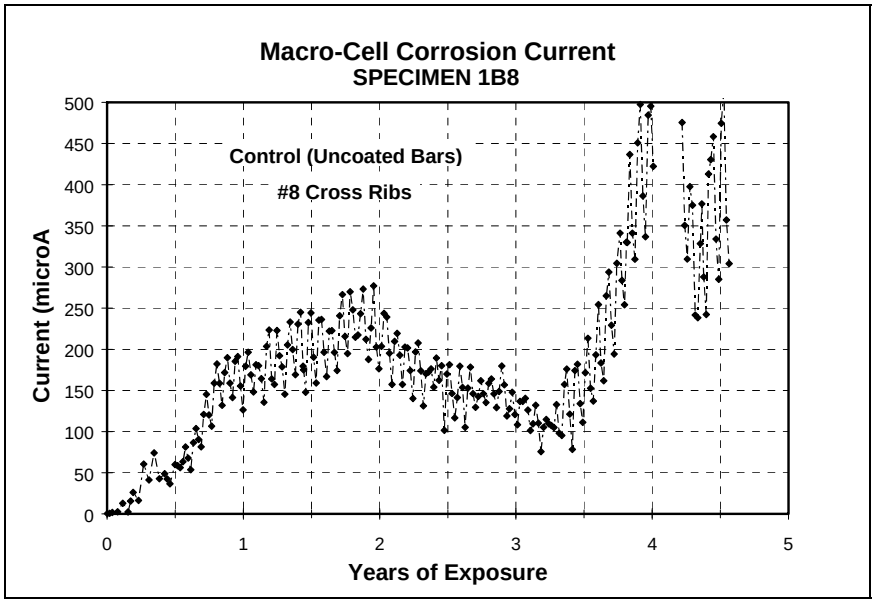

Figure 2.20. Macro-Cell Corrosion Current Readings for Specimen 1B8.

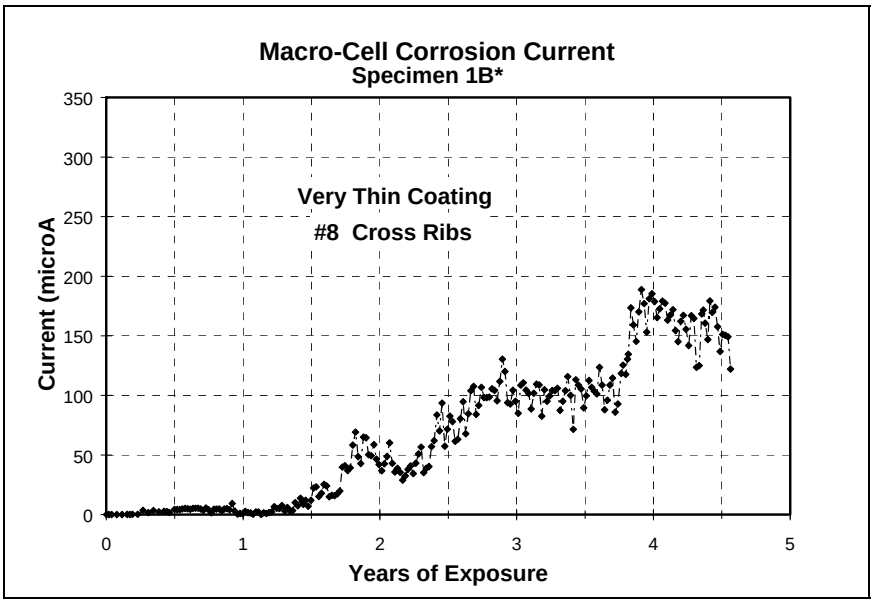

Figure 2.21. Macro-Cell Corrosion Current Readings for Specimen 1B*.

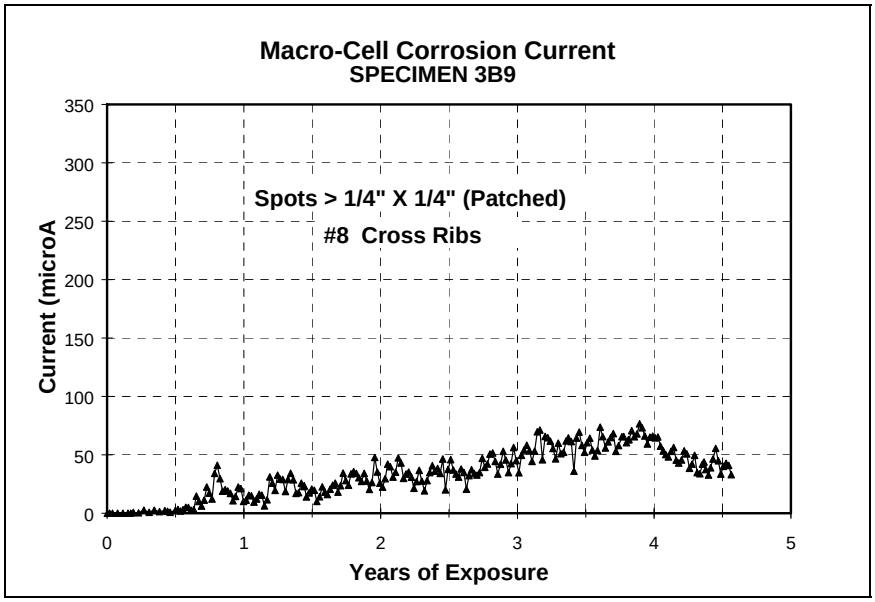

Figure 2.22. Macro-Cell Corrosion Current Readings for Specimen 3B9.

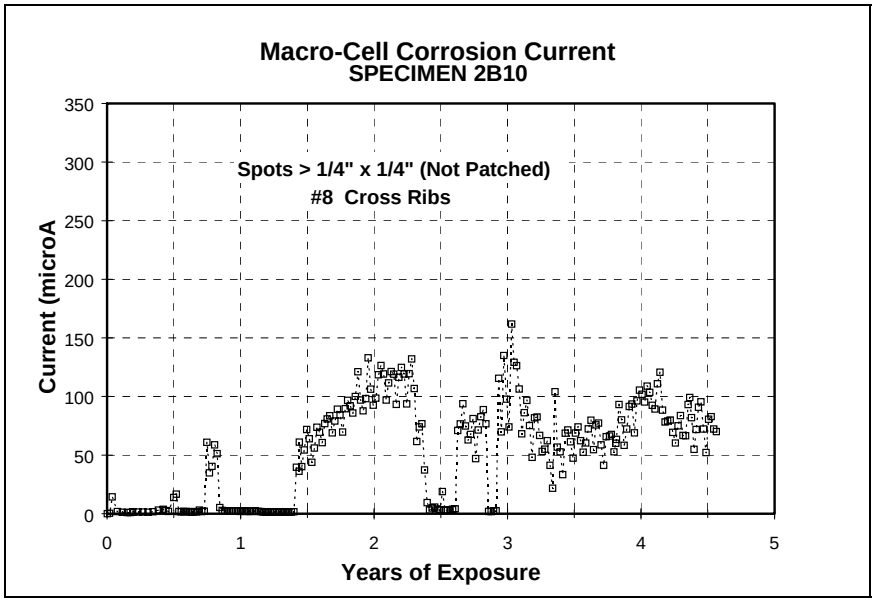

Figure 2.23. Macro-Cell Corrosion Current Readings for Specimen 2B10.

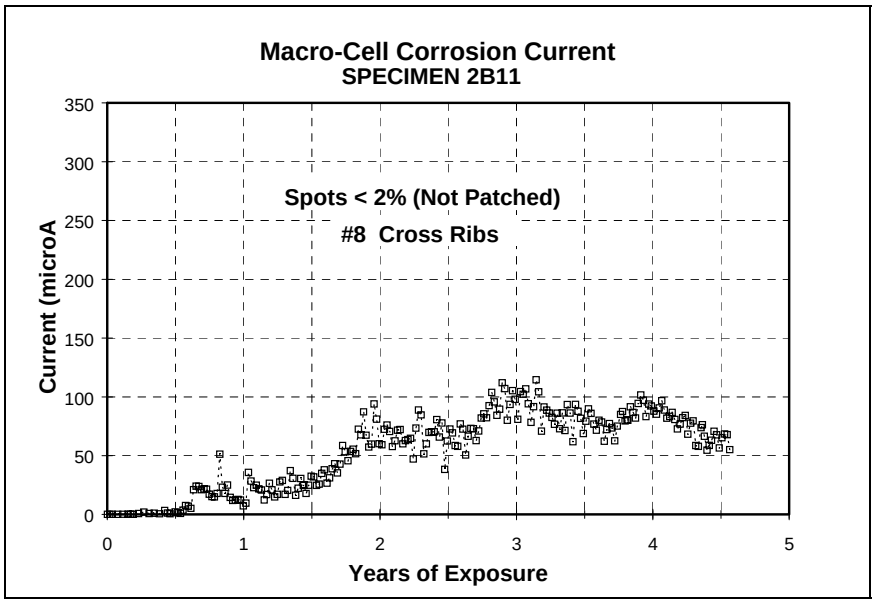

Figure 2.24. Macro-Cell Corrosion Current Readings for Specimen 2B11.

CHAPTER 3

ENCAPSULATION AND EPOXY INJECTION PROCESS

3.1 ENCAPSULATION AND EPOXY INJECTION OF BEAMS

The encapsulation and epoxy injection of beams was performed in a ten step Hardshell-CSRS Process. Properties of the materials are given in Appendix A.

3.1.1 Plate And Angle Fabrication

The plates and angles, which were E-glass fiber reinforced composites, were prefabricated in a controlled facility using the SCRIMP (Seemann Composites Resin Infusion Molding Process) vacuum infusion process. Installation time was reduced by pre-measuring the structure for exact cutting dimensions. Executing this cutting process in the shop eliminates on-site machining.

Plates and angles were sandblasted for better adhesion and felt stripping was attached to one side (Figure 3.1). The felt was used to create a space between concrete surface and the shell and serves as a bond line or channel for the adhesive to flow over the entire element. The felt stripping was laid out in specific patterns designed to promote or inhibit flow to specific areas.

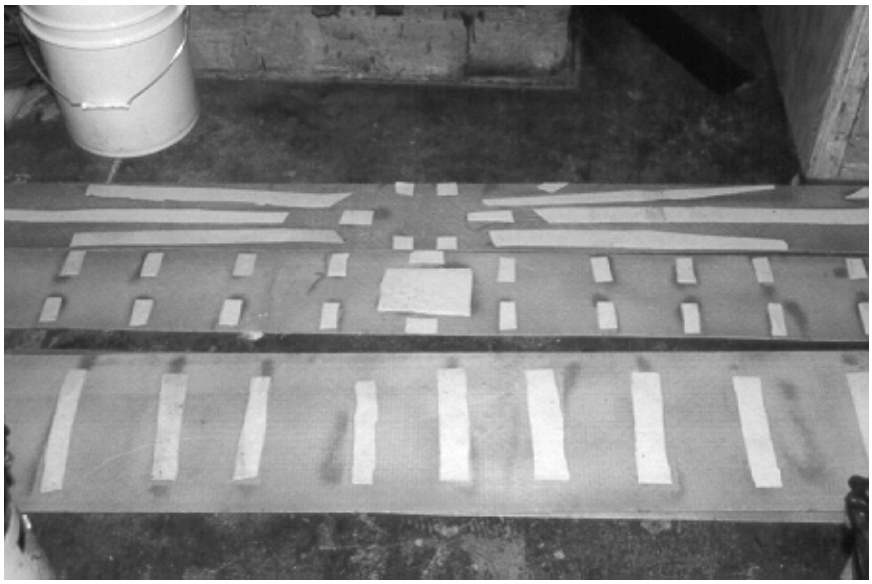

Figure 3.1. Felt Strips Attached on Side, Top, and Bottom Plates.

3.1.2 Concrete Surface Preparation

The concrete surface was prepared by pressure washing or grit blasting in order to provide a suitable surface for the adhesive system (Figure 3.2). The new material will not bond to the existing concrete surface unless the laitance produced by fine particles which may be carried to the surface by bleed water is removed to create a sound concrete surface.

3.1.3. Application of Distribution Media

A distribution media was applied at the ends of the beams in order to provide uniform epoxy flow (Figure 3.3).

Figure 3.2. Beams Cleaned and Distribution Media Placed at Ends.

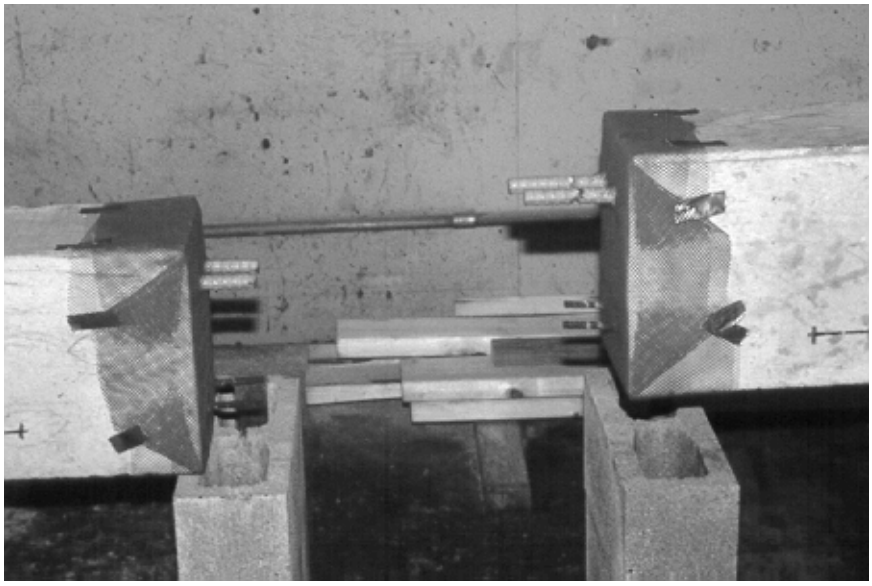

Figure 3.3. Application of Distribution Media.

3.1.4 Plate And Angle Installation

The plates and angles were tacked with a quick dry adhesive to hold them in place against the concrete so that the waterproofing membrane could be applied and the permanent adhesive infused.

Plates were erected in groups of opposing pairs (Figure 3.4) using quick dry adhesive and then held in place using prefabricated wood jigs and pipe clamps (Figure 3.5). Angles, because of their shape were more easily installed using the quick dry adhesive (Figure 3.6).

Figure 3.4. Erection of Plates.

Figure 3.5. Temporary Usage of Wood Jigs and Pipe Clamps.

Figure 3.6. Installation of Angles.

3.1.5 Injection Ports

After the placement of plates and angles was completed, injection ports were installed on top and bottom of the beams to draw a vacuum and to inject resin (Figures 3.7, 3.8).

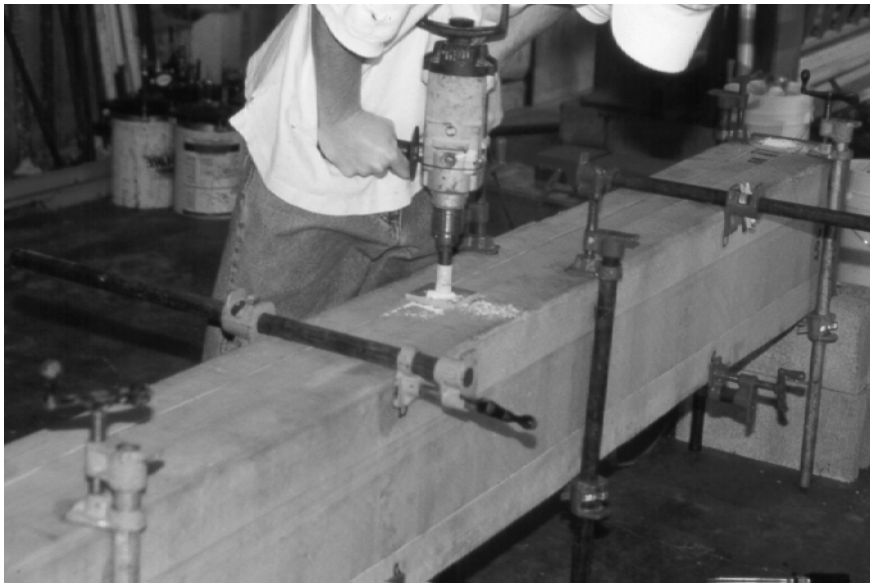

Figure 3.7. Installation of Injection Ports.

3.1.6 Airtight Waterproofing Membrane

In order to evacuate the volume inside the shell, an airtight seal must be provided over the plate and angle system. In the laboratory, plastic bags were used to provide a seal (Figure 3.9). The ends of the bags were sealed using tackey tape which was also used as a temporary patching material if a leak was found after evacuation has started.

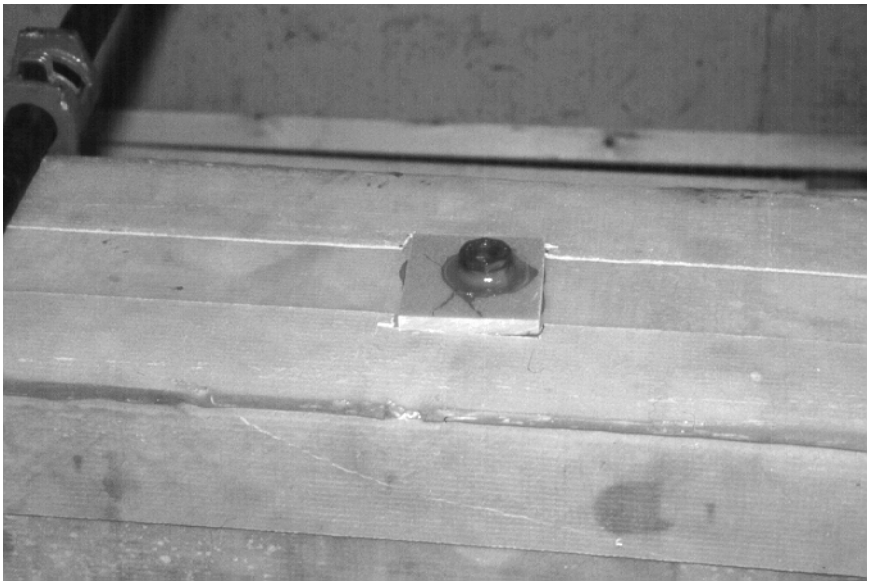

Figure 3.8. Installed Injection Port.

Figure 3.9. Application of Plastic Bags.

Under field conditions, an airtight seal would be provided using "Eliminator S" produced by Sterling Lloyd. Eliminator S is an acrylic based polymer spray on liquid that hardens within 45 minutes even in cold temperatures. It also provides an environmental coating that protects the composite wrapping against UV light and moisture.

3.1.7 Infusion Preparation

The composite encased concrete was fitted with feeder inlets (Figure 3.10). The inlets were placed strategically to ensure quick and complete infusion. The encapsulated element was then evacuated and a leak test was performed to check the integrity of the seal (Figure 3.11). Perfect vacuum was rarely achieved immediately after the vacuum was drawn. Leak checks were performed and leaks were sealed with temporary patching materials such as tackey tape (Figure 3.12). These patches were removed following the infusion. The structure remained in a vacuum of 27 inches of mercury to remove excessive moisture in concrete. The system was then ready for infusion.

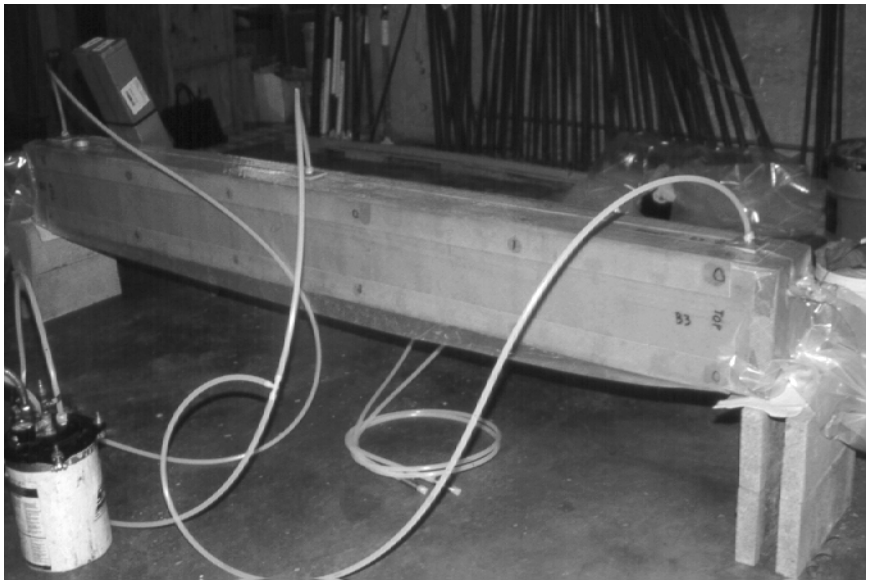

Figure 3.10. Feeder Inlets.

Figure 3.11. Evacuation Process.

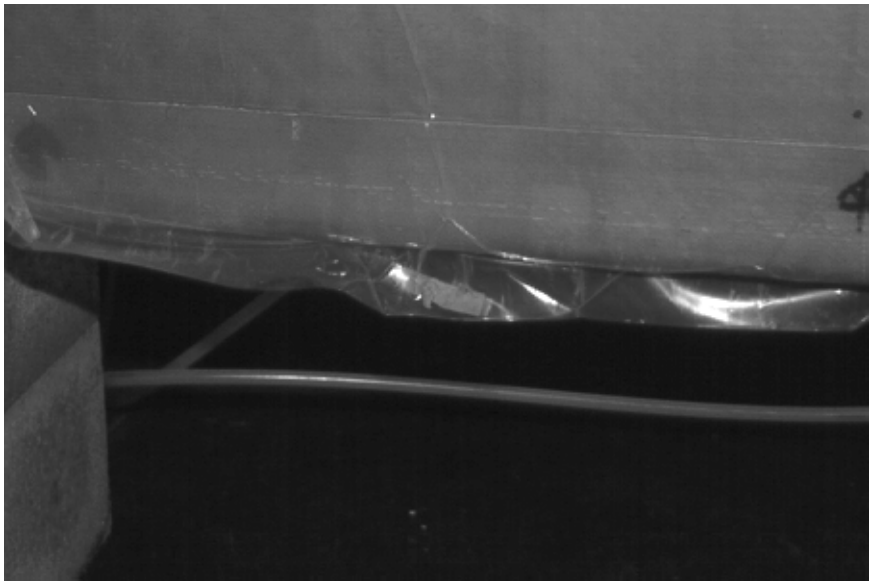

Figure 3.12. Using Tackey Tape as a Patching Material.

3.1.8 Mixing the Resin

Once the system was ready for infusion the resin was mixed (Figure 3.13). Dow Derakena 8084 epoxy vinyl ester resin was used for this application. Cobalt Napthenate 6% was added to the resin at 0.4% by volume. After Cobalt Napthenate was fully mixed with the resin, Trigonox 239A was added at 2% by volume and mixed. These concentrations were related to give the desired gel time for infusion.

3.1.9 Infusion

The system was designed to draw resin from the bottom inlet ports, up through the structure, and out through the top vacuum ports (Figure 3.14).

Figure 3.13. Mixing the Resin.

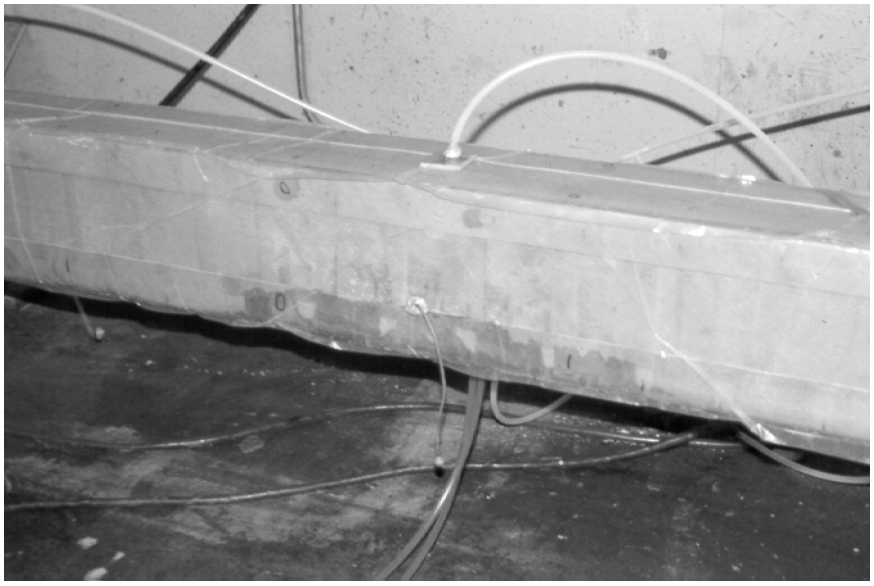

Figure 3.14. Infusion Process (Epoxy Injection).

The felt strips directed the flow so that the entire structure was infused (Figure 3.15). Vacuum remained on the system for 24 hours until the adhesive reached its specified mechanical properties (See Appendix B).

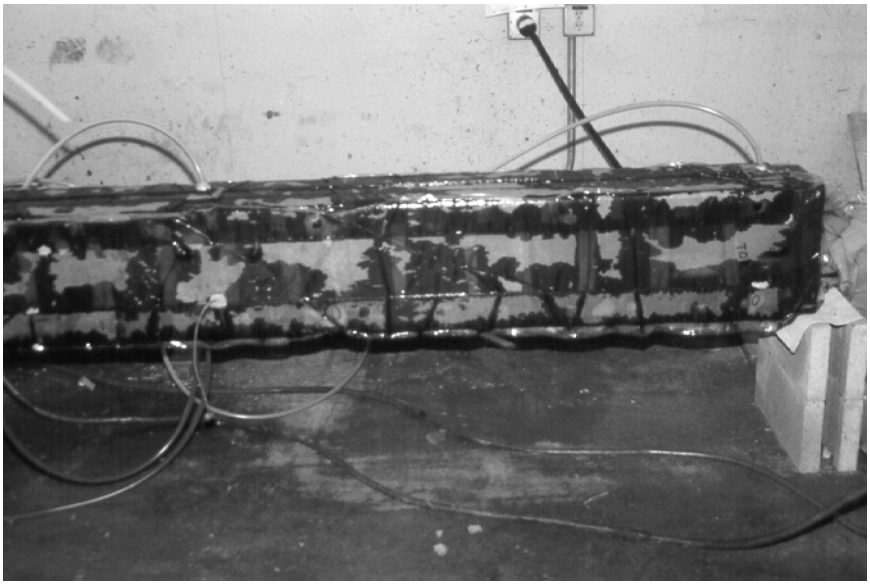

Figure 3.15. End of Encapsulation and Epoxy Injection Process.

3.1.10 Post Infusion Clean-up

In the field, following the 24 hour curing period, all the hoses are removed. The port holes are permanently patched as are spots where temporary patches were installed during the leak checks. A coating of “Eliminator S” is then applied to the patched areas for both waterproofing and aesthetics.

In the laboratory, all the hoses were removed and the beams were taken out of the plastic bags after the 24 hour curing period.

3.2 ENCAPSULATION AND EPOXY INJECTION OF MACRO-CELLS

The encapsulation and epoxy injection process for the macro-cells was performed simultaneously with the beams. Since the macro-cells were small, no hardshell encapsulation was provided after the surface of the macro-cells was prepared as described in Section 3.1.2. The same distribution media used for the beams was applied all around the macro-cells in order to provide a uniform resin flow (Figure 3.16).

Figure 3.16. Application of Distribution Media.

After the placement of the distribution media, injection ports were installed at top and bottom of the macro-cells. Omega channels were used as injection ports for macro-cells (Figure 3.17). The macro-cells were placed in plastic bags and the ends of the bags were sealed using tackey tape (Figure 3.18).

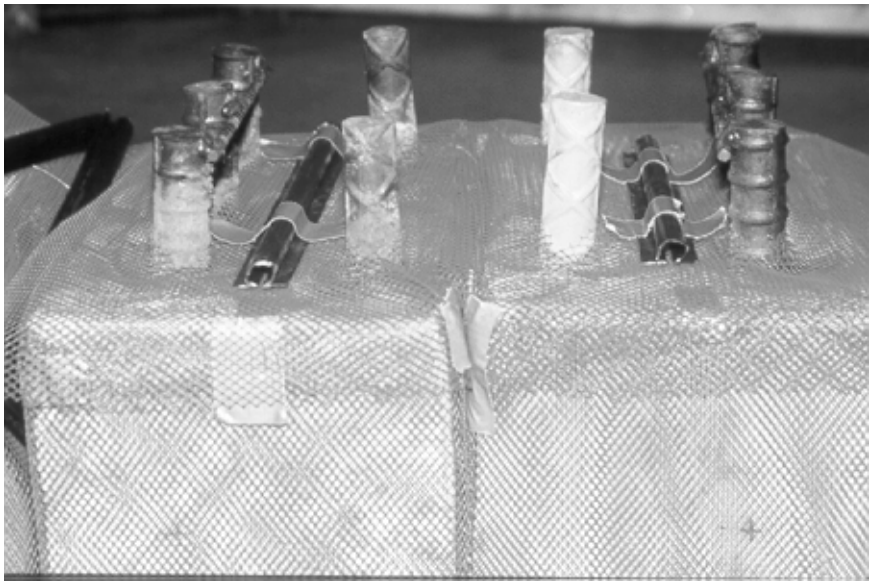

Figure 3.17. Application of Omega Channels as Injection Ports.

After the airtight seal was applied, the feeder inlets were installed (Figure 3.19). As in the case of the beams, leak checks were performed and leaks were sealed with tackey tape. After 24 hours of evacuation at 27 inches of mercury, the system was ready for infusion (Figure 3.20). The resin mixed for the beams was used for infusion of the macro-cells as well. The system was designed as in the beams to draw resin from the bottom inlet ports, up through the structure, and out through the top vacuum ports (Figure 3.21).

Once the adhesive hardened, the infusion process was complete (Figure 3.22). As in the beams, vacuum remained on the system for 24 hours until the adhesive reached its specified mechanical properties. After a 24 hour curing period, all hoses were removed and the macro-cells were taken out of the plastic bags (Figure 3.23).

Figure 3.18. Application of Plastic Bags.

Figure 3.19. Application of Feeder Inlets.

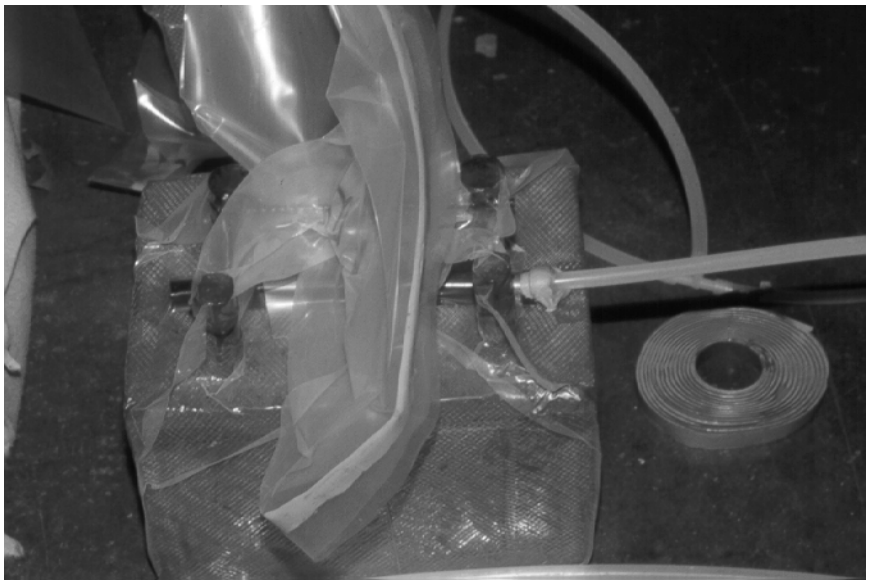

Figure 3.20. Evacuation Process.

Figure 3.21. Epoxy Injection.

Figure 3.22. End of Process.

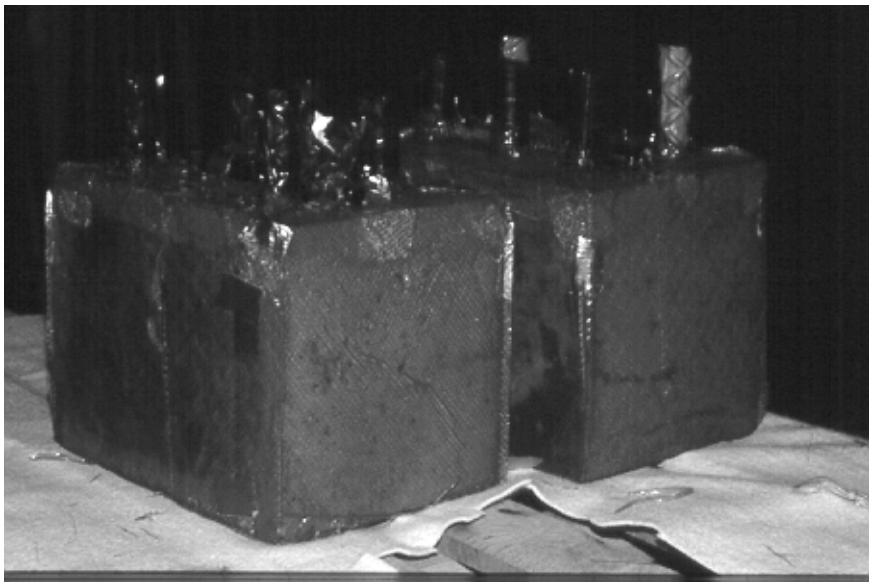

Figure 3.23. Post Infusion Clean-up.

CHAPTER 4

TEST SETUP AND MONITORING

4.1 BEAMS

4.1.1 Exposure and Test Setup

The beams were exposed to a 3.5% saline solution. The same solution was used in the previous study. Exposure time and beam surface area exposed were different than in the previous study. Each exposure cycle consisted of a one week wet period followed by three week dry period. Rather than exposing a defined area, the entire beam surface was exposed in order to assess the effectiveness of encapsulation. During the wet cycle, the corrosive solution was circulated over the beams continuously and then the beams were allowed to air dry for three weeks. Cloth was placed on the beams during the wet cycle in order to provide more uniform exposure over the entire beam since the corner plates of encapsulated beams formed a channel for water to flow and prevented the sides of the beams from exposure (Figure 4.1). A total of thirteen cycles were applied to the beams.

In order to apply the exposure described above, a retaining pool was designed. Figure 4.2 shows the details of the retaining pool and the test setup for the beams. The retaining pool was fabricated using plywood sheets, a

polyurethane sheet on the bottom which extended partially along the sides and served as the catch basin for the solution, and the remainder of the plywood was covered with plastic sheets in order to protect the plywood. The polyurethane sheet was placed on an existing elevated slab. A drain in the base of the pool was connected to a pump which recirculated the water to the top of the beams through a distribution system of PVC pipes. Holes were drilled into the bottom of the PVC pipes to distribute the saline solution over the length of the beams.

The beams were placed on wood stands inside the pool to keep them above the collected water. Figure 4.3 shows the placement of the beams on the stands. Figure 4.4 shows the retaining pool, the recirculation pump, and the PVC distribution pipes.

Figure 4.1. Cloth on Beams.

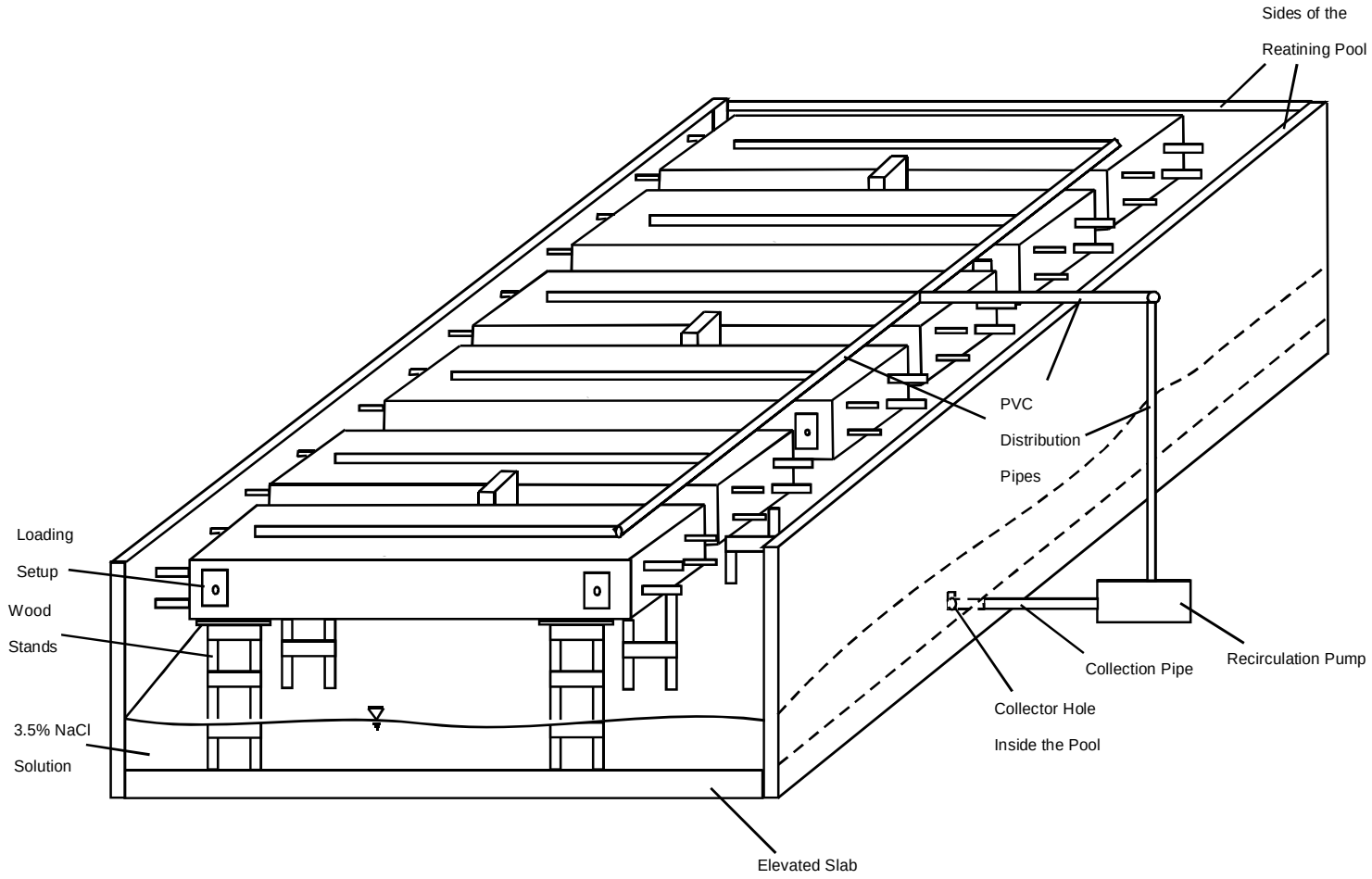

Figure 4.2. Test Setup for Beams.

Figure 4.3. Placing the Beams on Wood Stands in the Retaining Pool.

Figure 4.4. Retaining Pool, Recirculation Pump, and PVC Distribution Pipes.

4.1.3 Loading

Before the start of the exposure cycles, the encapsulated beams were loaded to reach two thirds of the yield stress in order to crack the concrete but not yield the bar. The load-deflection plot is shown in Figure 4.5. Cracking was desired in order to fully test the effectiveness of the encapsulation process in a situation where loads on the structure may be sufficient to crack the concrete.

Once the exposure study started, four of the six beams (two encapsulated, two control beams) were loaded back to back, while two were not loaded. The loading setup is shown in Figure 4.6. Each week the load on the loaded beams was removed. Then the beams were loaded and unloaded 5 times. The last loading remained on the beams to keep the cracks open as was done in the previous study. The beams were subjected to the same level of load as in the previous study.

The beams were loaded back to back as simple beams with peak moment at the center. As a result, cracking was concentrated near the mid-span where the stirrup was located.

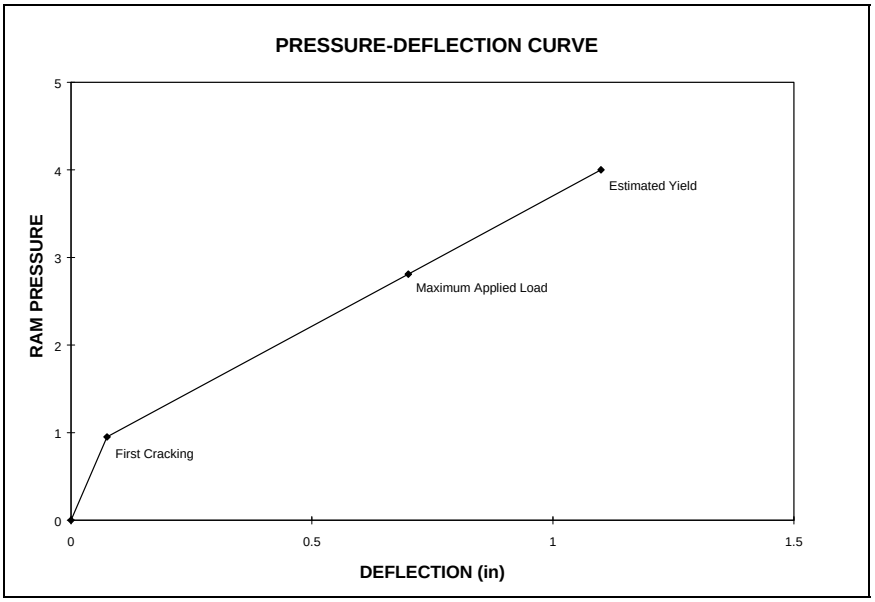

Figure 4.5. Beam Pressure-Deflection Prior to Exposure.

Figure 4.6. The Loading Process.

4.1.4 Monitoring

For the duration of the project (1 year) the beams were monitored by taking half-cell potential readings against saturated calomel reference electrode (SCE). The readings were taken weekly for the control specimens while they were taken every 3 months for the encapsulated ones. The 3 month intervals were preferred in order not to disturb the continuity of the encapsulated beams. Figures 4.7 and 4.8 show the process for taking half-cell potential readings for unencapsulated and encapsulated beams respectively. For the encapsulated beams, a number of access holes through the fiber composite were provided along the beams at the level of the bars in order to access the concrete surface for half-cell potential measurements. The holes were limited in number in order to avoid disturbing the continuity of the encapsulated beams. Figure 4.9 shows the access holes on encapsulated beams. After taking the readings, the access holes were sealed using silicon. When the access holes were opened in order to take the readings a clear fluid was found inside the holes. The fluid was collected and analyzed; the results are discussed in Chapter 5. For the control specimens, readings were continued as before since the surface could be accessed at the same locations as in the previous study.

In addition to half-cell potential measurements, acoustic emission testing was performed on the beams in order to determine the applicability of that technique for corrosion monitoring. The procedure for acoustic emission application is discussed in Appendix B.

Figure 4.7. Taking Macro-Cell Readings for Unencapsulated Beams.

Figure 4.8. Taking Macro-Cell Readings for Encapsulated Beams.

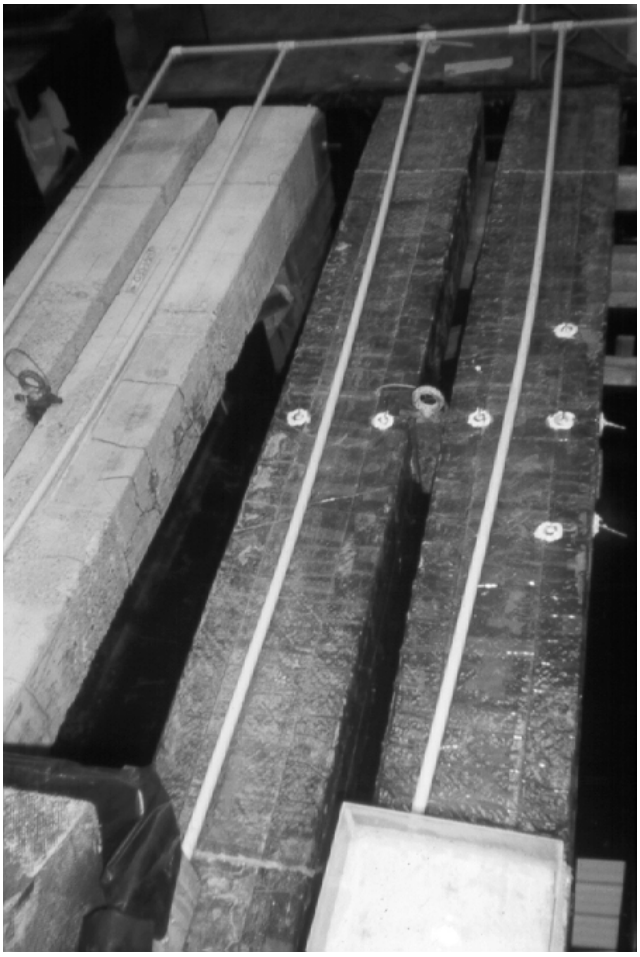

Figure 4.9. Access Holes on Encapsulated Beams.

At the end of the exposure period, core samples were taken from the encapsulated beams to assess the depth of resin impregnation (Figure 4.10). The beams were autopsied to assess the condition of the bars and the concrete around the bars. Finally, the bars were removed from concrete. The results from the monitoring processes and the autopsies are discussed in Chapter 5.

Figure 4.10. Taking Core Samples.

4.2. MACRO-CELLS

4.2.1 Exposure and Test Setup

Like the beams, the macro-cells were exposed to a 3.5% by weight NaCl solution.

In the case of macro-cells, the exposure cycles consisted of a 2 week wet period followed by a 2 week dry period. This was the same exposure cycle used for the previous study. The test setup for the encapsulated macro-cells was designed help understand the effectiveness of the encapsulation and epoxy injection procedure. During the wet period, the encapsulated macro-cells were placed upside down inside a small retaining pool that had a 30º angle with the horizontal and the pool was filled with the saline solution. When the wet period ended, the specimens were taken out of the water. In this way the corners which are harder to seal using epoxy would also be exposed and the effectiveness of the resin used in encapsulation could be studied. The control specimens were ponded just as they had been for the last 5 years. Thirteen exposure cycles were completed during this study. Figure 4.11 shows the retaining pool and the test setup for the encapsulated macro-cells and Figure 4.12 shows the test orientation both encapsulated and control macro-cells.

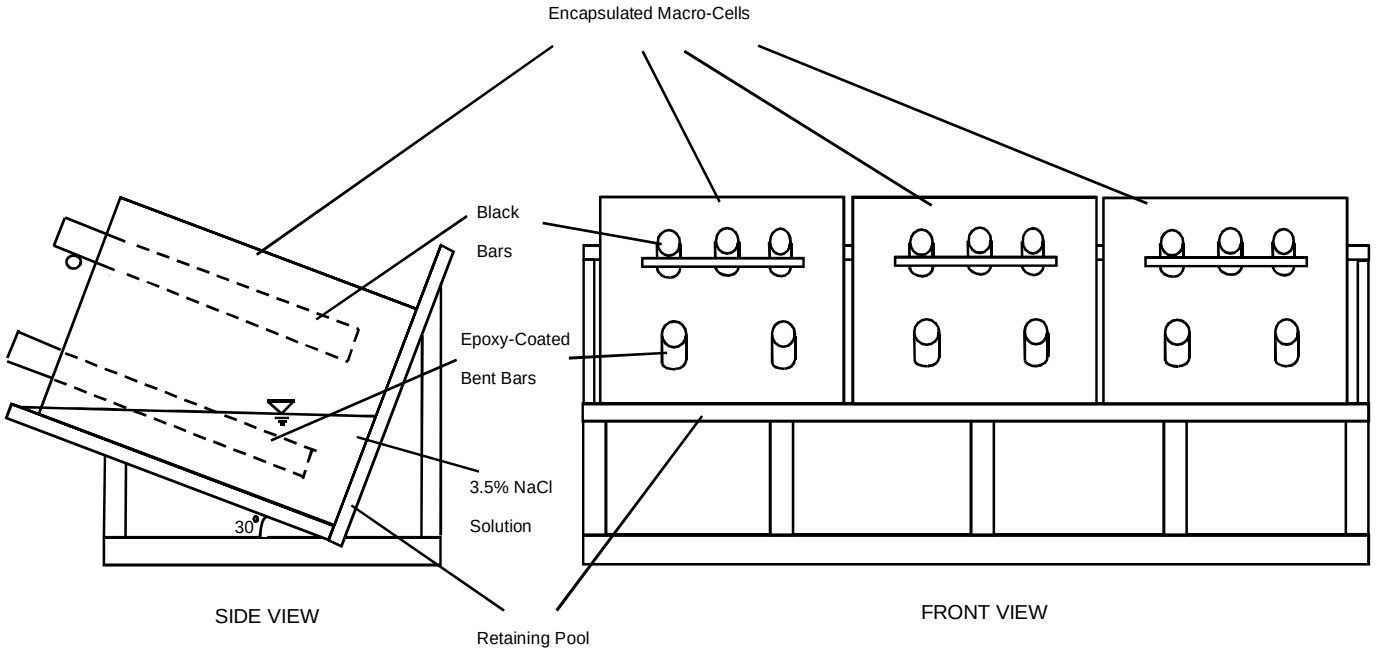

Figure 4.11. Retaining Pool and Test Setup for Encapsulated Macro-Cells.

Figure 4.12. Test Orientation for Macro-Cells.

4.2.2 Monitoring

All macro-cells were monitored by taking potential readings twice a week. Top and bottom reinforcing layers were linked using a 100ohm resistor. The voltage drop across the resistor was measured with a voltmeter and the voltage was converted to current using Ohm's Law. However, some readings might have changed slightly during this process since the wires connected to the data acquisition system in the previous study changed the resistance.

In addition to macro-cell potential readings, the control specimens were monitored by taking half-cell potential readings against SCE each week. This could not be done for the encapsulated macro-cells since there was no access to the concrete surface.

At the end of the exposure cycles, the macro-cells were opened to assess the condition of the bars and the concrete, and the penetration of the resin. Finally, the bars were removed from concrete. The results from the monitoring processes and the autopsies are discussed in Chapter 5.

CHAPTER 5

TEST RESULTS AND DISCUSSIONS

5.1 BEAMS

5.1.1 Half-Cell Potentials

The half-cell potentials throughout the duration of the encapsulation study as well as the previous study are shown in Figure 5.1 through 5.6. The previous study is shown as the TxDOT Program and the encapsulation study is shown as Encap. Program. There was a gap of 6 months between the two studies as shown. As described in Chapter 2, in the graphs, black bar refers to the uncoated bar, epoxy 1 to the "upper" epoxy-coated bar when the beams are in exposure position (on their side), and epoxy 2 to the "lower" epoxy-coated bar in the exposure position (Figure 2.6).

It is seen from the half-cell potential results that the readings for the control specimens have a tendency to become more negative while the readings for the encapsulated specimens tend to stay at the level they were before encapsulation. The tendency towards more negative values for the control specimens (Beams 12 and 30) might be due to a change in the humidity during the dry period. In the test setup, the beams remained supported above the pool of

water. Evaporation from the pool may have raised the humidity in comparison with the previous study.

The encapsulated specimen readings remained at the level they were before. Encapsulation could provide a barrier protecting the beam from addition external exposure. However, with readings remaining at the same level indicates that the evacuation procedure for removal of moisture from the specimens was not successful and the moisture, oxygen, and chlorides left inside the specimens allowed corrosion to continue. In the following sections, the results from acoustic emission testing, and from opening of the beams are discussed in terms of the processes discussed above.

One important point to be mentioned is that the half-cell potential readings show a 90% or higher probability of corrosion as discussed in Chapter 2. It was found by the end of the previous study, however, that there is no direct correlation between the hall-cell potential readings and the amount of corrosion damage inside the beams. That is, corrosion in a beam showing more negative values is not necessarily worse than corrosion in a beam showing less negative if both readings are above a certain threshold (-275 mV.) [Vaca, 1998].

The fluid found in the access holes of the encapsulated specimens described in Chapter 4 was analyzed using Mass Spectrometry. The results indicated that the fluid was different from the saline solution and contained organic products. This finding eliminated the concern that the seals around the access holes were leaking and it was concluded that the fluid was coming to the

surface from the interior of the beams and moisture in the concrete was not removed during the evacuation process prior to encapsulation.

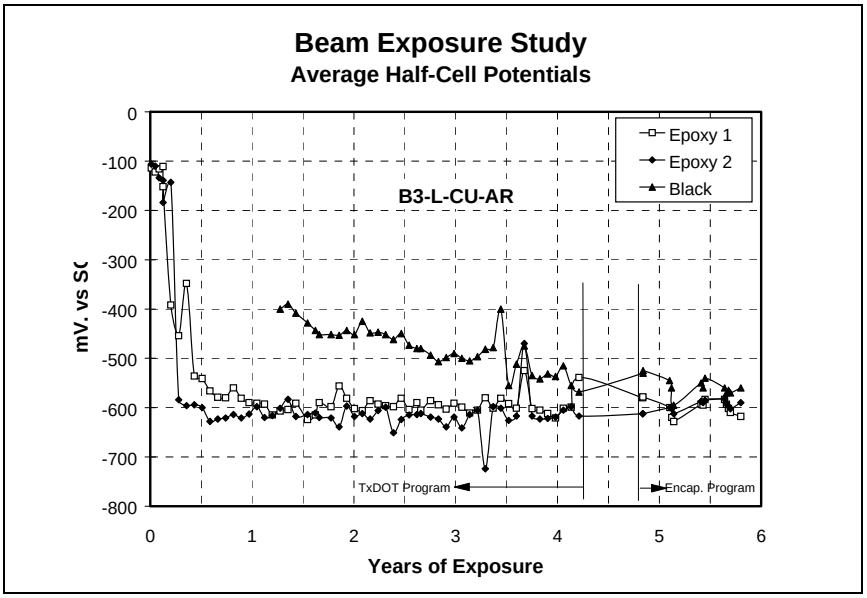

Figure 5.1. Half-Cell Potential Readings for Beam 3.

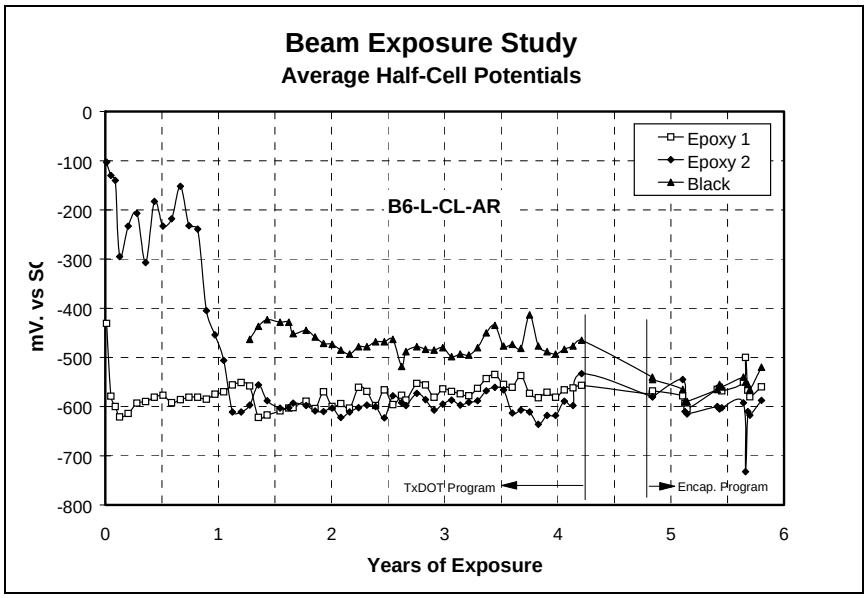

Figure 5.2. Half-Cell Potential Readings for Beam 6.

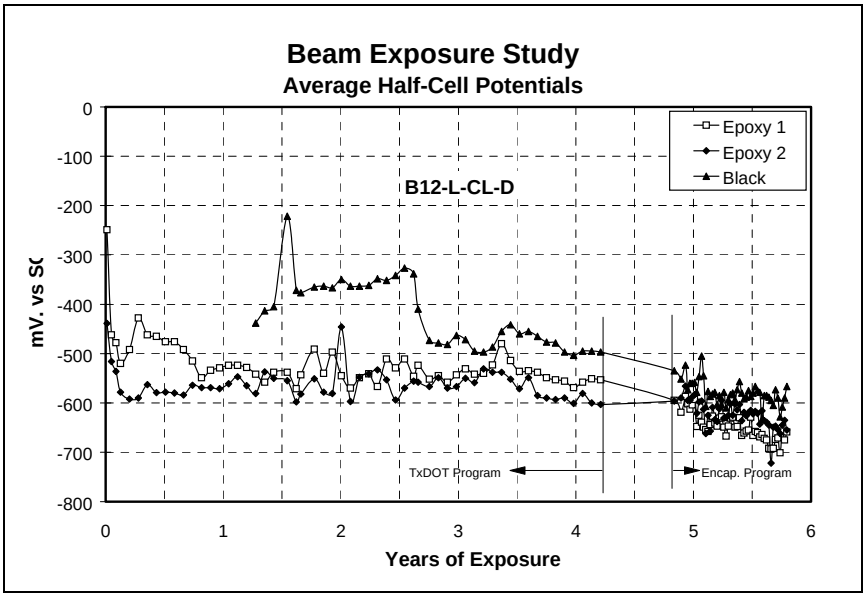

Figure 5.3. Half-Cell Potential Readings for Beam 12 (Control).

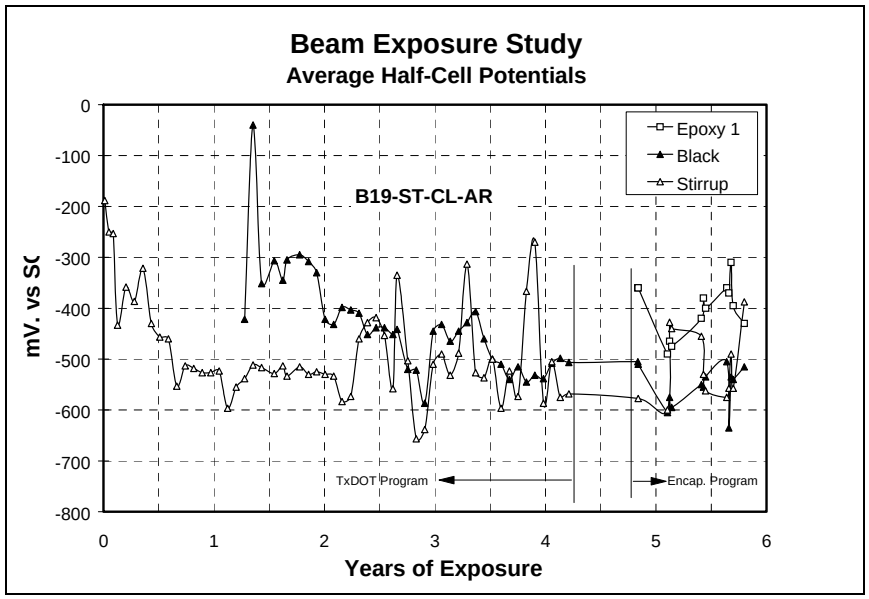

Figure 5.4. Half-Cell Potential Readings for Beam 19.

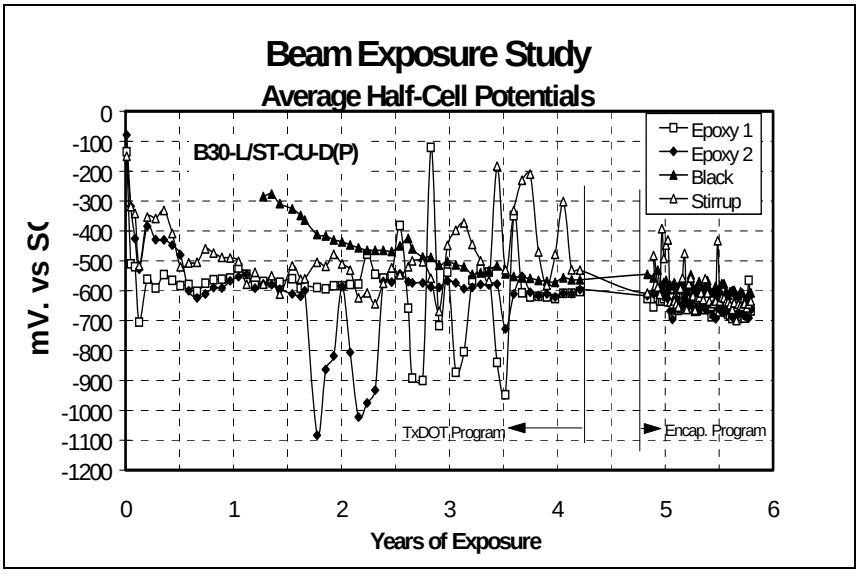

Figure 5.5. Half-Cell Potential Readings for Beam 30 (Control).

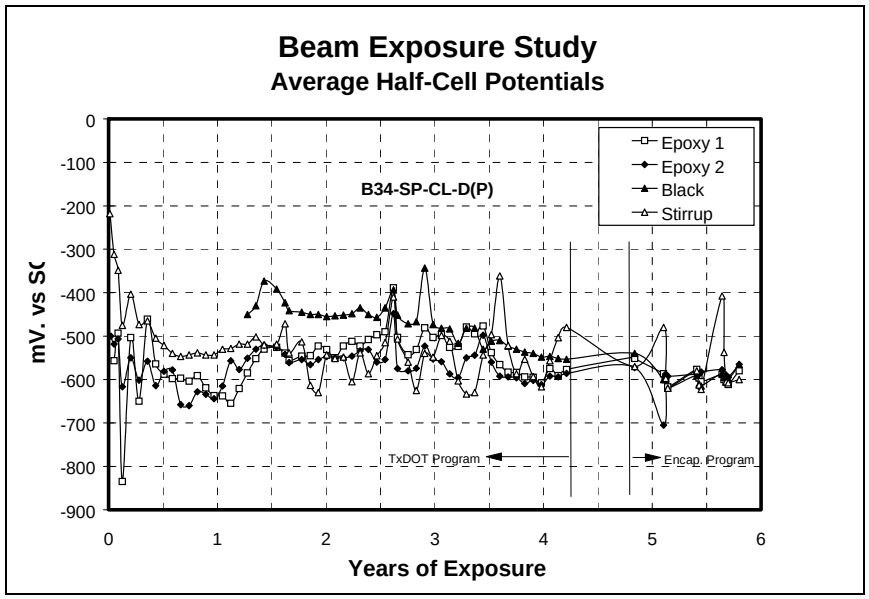

Figure 5.6. Half-Cell Potential Readings for Beam 34.

5.1.2 Acoustic Emission Testing

Acoustic emission techniques were used to monitor corrosion inside the beams on a trial basis. The results were very encouraging and are discussed in Appendix B.

5.1.3 Chloride Content

Results from the chloride content analysis of the beams after completion of exposure testing are compared with the results from the previous study in Table 5.1. The chloride samples for this study were taken from the previously exposed area shown as the “Wet Zone”, just outside this area shown as “Dry Zone”, and at

the end of the beams shown as “End” in Table 5.1. These readings were compared with the readings from the “Wet Zone” in the previous study. It is seen from this data that the levels had changed some but they are similar in the “Wet Zone”. The differences are likely due to variability of data within a beam and sampling errors. Some chlorides may have been depleted due to corrosion continuing inside the encapsulated beams. Chloride contents above the threshold for corrosion (0.02%-0.05%) were found at the ends of all the beams except for one beam. Corrosion was observed at the ends of the beams as discussed in the following section.

Table 5.1. Summary of Chloride Content Testing.

		Chloride Content (%)			
		Previous Study	**This Study**		
Beam	**Depth (mm)**	**Avg. Wet Zone**	**Avg. Wet Zone**	**Avg. Dry Zone (Near Wet Area)**	**Avg. at End**
B3	50-75	0.46	0.50	0.55	0.04
	127-152	0.67	0.61	0.74	0.07
B6	50-75	0.77	0.51	0.47	0.03
	127-152	0.88	0.52	0.40	0.07
B12	50-75	0.51	0.56	0.45	0.08
	127-152	0.61	0.56	0.64	0.04
B19	50-75	0.72	0.49	0.06	0.00
	127-152	0.65	0.41	0.14	0.00
B30	50-75	0.74	0.55	0.30	0.03
	127-152	1.06	0.57	0.48	0.05
B34	50-75	1.07	0.44	0.53	0.10
	127-152	0.88	0.85	0.33	0.05

5.1.4 Core Samples and Autopsies

Before the beams were opened for making autopsies, core samples were taken to assess the depth of resin impregnation. From the core samples, it was found that there was no epoxy penetration except at the crack locations where some cracks were partially filled. Some cracks without any resin penetration were found during the assessment of the cores. It was also found that voids near large cracks were not impregnated.

To pursue the idea of resin impregnation, additional testing was done. Six plain concrete blocks of 8in x 12in x 12in were cast in order to test the effectiveness of resin impregnation. Two of these blocks were kept saturated, two were kept air dried, and two were oven dried before applying the encapsulation and epoxy injection process described in Chapter 3. After encapsulation, core samples were taken from the specimens to determine the resin impregnation from the surface. It was found regardless of curing conditions of the specimens that the resin impregnation through the concrete was not accomplished unless there was a surface cracking due to shrinkage and temperature effects and in most cases the resin only formed an outside layer and did not penetrate the concrete at all.

The inspection of the core samples were performed under ultraviolet light since the epoxy penetration was not visible to the bare eye but glowed under ultraviolet light.

When the beams were opened , a green corrosion fluid, generally indicative of active corrosion was found along the black (uncoated) bars in all beams. The amount and viscosity of this fluid however, changed from beam to

beam. Figures 5.7 and 5.8 show this corrosion fluid on beams 30 and 34 respectively.

A difference in color of the concrete at previously exposed areas and the rest of the beam was consistently found in encapsulated specimens (Darker area to the right in Figure 5.9). The “wet” appearance indicated that moisture remained inside the beams and, as a consequence, half-cell potential readings remained stable. Corrosion activity was continuing inside the beams as before encapsulation.

Figure 5.7. Green Corrosion Fluid on Beam 30.

Figure 5.8. Green Corrosion Fluid on Beam 34.

Figure 5.9. Difference in Appearance of Concrete in Beam 3.

Another observation was that the epoxy coated bars usually performed well while the uncoated bars were severely corroded. Beam 34, which had spliced bars, was the only beam with damage to epoxy coated bars. The end of the bars where epoxy was patched were corroded. Other than that, visible damage to the epoxy coated bars was insignificant. There were some stains near the stirrup in all the beams. The stains were probably caused by corrosion of tie wire. In some cases the corrosion extended underneath the epoxy coating and was found only after the epoxy coating was peeled away. The bar surface was mottled with rust. The locations where corrosion was observed under the coating generally corresponded with the locations of splices, intentionally damaged areas on epoxy coating , intentionally damaged and patched areas on epoxy coating, and crack locations. Figure 5.10 shows how well the epoxy coated bars performed. Figures 5.11 and 5.12 show the rust stains on and underneath the epoxy coating. Figure 5.13 shows the damage underneath the epoxy coating for Beam 12, while the same bar is seen without any damage in spite of the intentional damage shown in Figure 5.14. These differences were primarily related to crack locations.

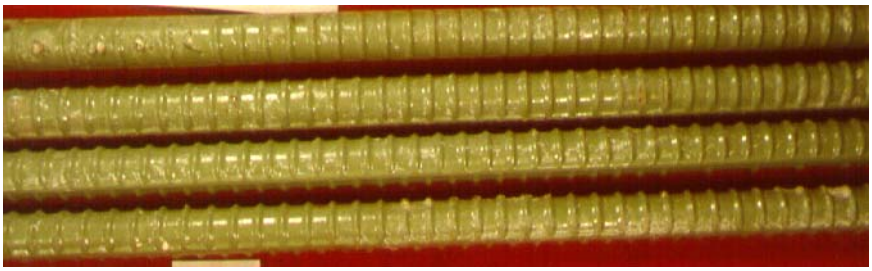

Figure 5.10. Epoxy Coated Bars (Beam 34).

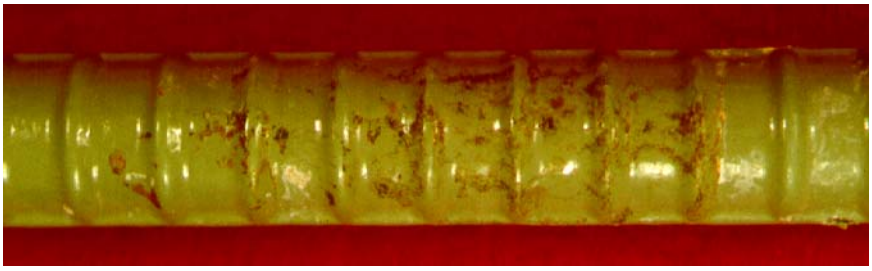

Figure 5.11. Rust Stains on Epoxy Coated Bar (Beam 6).

Figure 5.12. Rust Stains Underneath Coating on Epoxy Coated Bar (Beam 6).

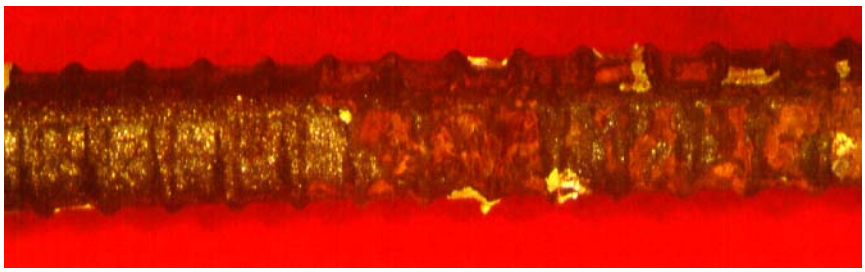

Figure 5.13. Rust Stains Underneath Coating on Epoxy Coated Bar (Beam 12).

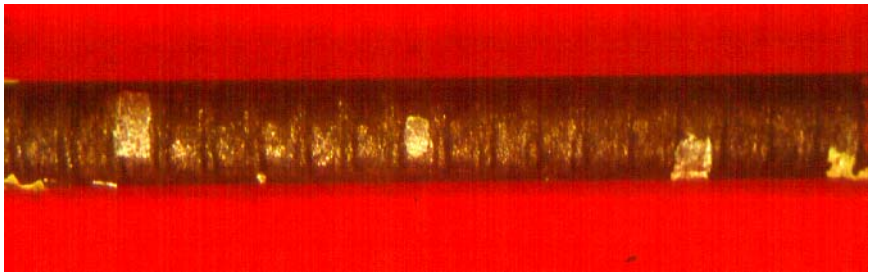

Figure 5.14. No Damage Underneath Coating on Epoxy Coating Bar (Beam 12).

In the uncoated bars of all beams, significant loss of steel areas as well as pitting in several locations was observed. Significant loss of steel area is shown in Figure 5.15 for Beam 19 bottom black bar near stirrup, in Figure 5.16 for Beam 6 bottom black bar in the previously exposed region, and in Figure 5.17 for Beam 12 top black bar in the previously exposed area. The loss of bar area shown was typical of the black bars of all the beams. Significant loss of bar area is defined as loss of more than 15-20% of the bar area. For the control specimens, corrosion damage extended outside the previously exposed region in the form of pitting (Figures 5.18, 5.19). In pitting corrosion the profile of the bar remains the same. There are pits that do not significantly (less than 10%) change the bar area. For the encapsulated specimens the damage was usually within the previously exposed region. All of the encapsulated specimens, however, showed pitting corrosion at the end of the beams (Figures 5.20, 5.21). It is likely that the ends of the encapsulated beams were not sealed properly around the protruding bars and corrosion was initiated in regions where no corrosion had occurred earlier. Corrosion activity on the black bars in the encapsulated specimens appeared to be greater than the damage in the control (unencapsulated) specimens.

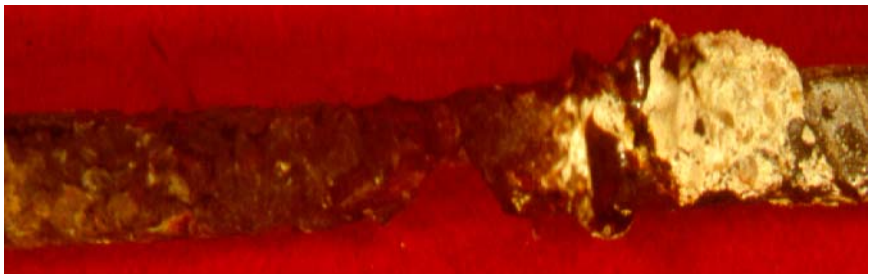

Figure 5.15. Significant Loss of Bar Area (Beam 19).

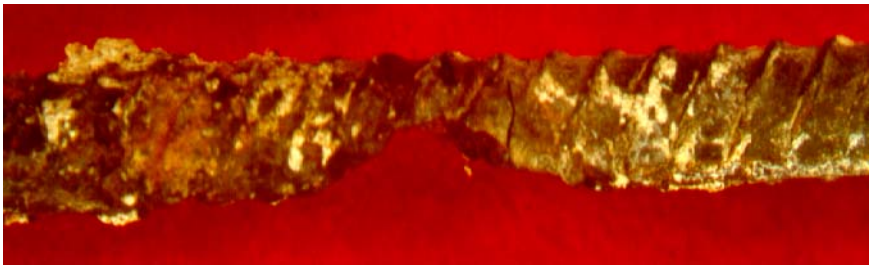

Figure 5.16. Significant Loss of Bar Area (Beam 6).

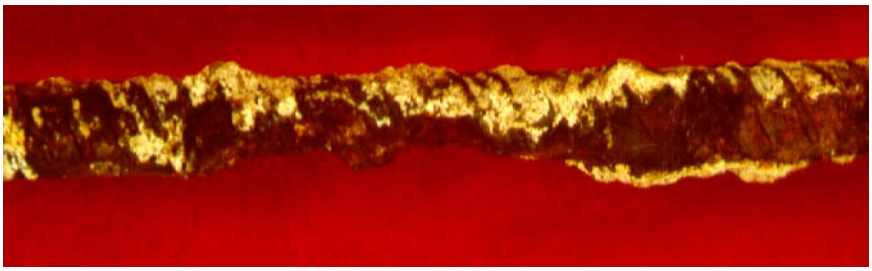

Figure 5.17. Loss of Bar Area (Beam 12).

Figure 5.18. Corrosion Outside the Previous Exposed Region (Beam 12).

Figure 5.19. Corrosion Outside the Previous Exposed Region (Beam 30).

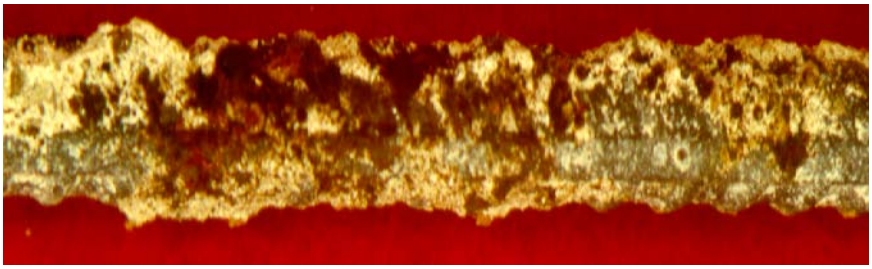

Figure 5.20. Pitting Corrosion at the End of the Bar (Beam 6).

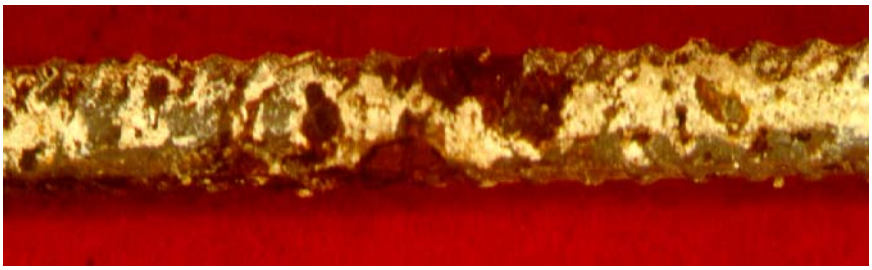

Figure 5.21. Pitting Corrosion at the End of the Bar (Beam 19).

In the three beams where the stirrups were monitored (B19, B30, and B34), significant corrosion damage was observed in the stirrups. There were stains on the epoxy coating and when the coating was peeled, the bars had a nearly total rusted surface. In the previous study it was found that the bars bent after coating did not perform well [Vaca, 1998]. Figures 5.22 and 5.23 show the stirrups after removal from the beams.

Figure 5.22. Corrosion Damage on Stirrup (Beam 30).

Figure 5.23. Corrosion Damage on Stirrup (Beam19).

Table 5.2. Summary of Damage Condition of Bars.

		Corrosion Damage		
Beam	**Type**	**Black Bars**	**Epoxy Coated Bars**	**Stirrup**
B3	Encapsulated	Significant loss of bar near stirrup and several other locations in PEA. Pitting at the end.	Bars in good shape. Only stains around the stirrup. Rust was found underneath these stains when epoxy coating was peeled. Insignificant damage.	Not applicable.
B6	Encapsulated	Significant loss of bar area and pitting in PEA. Pitting at the end as well.	Stains in the middle and in the PEA. When epoxy peeled some minor damage was found.	Not applicable.
B12	Control	Significant loss of bar area in PEA. Some pitting and mottled surface outside the PEA and at the end.	Stains at PEA, especially at intentionally damaged locations. Not all locations exhibited corrosion. Some pitting corrosion at PEA.	Not applicable.
B19	Encapsulated	Significant loss of bar area around the stirrup. Pitting at the end.	Not applicable.	Corrosion all around. Pits in the epoxy coating. Damage found especially at the bents when epoxy was peeled
B30	Control	Significant loss of bar area and pitting in several locations extending uniformly through the of bar.	Stains around the stirrup and at locations of patching. Rust was found underneath epoxy coating on these locations.	Coating peeled off in several locations. Bar underneath corroded. Stirrup extensively corroded.
B34	Encapsulated	Significant loss of bar area near the stirrup. Damage extending throughout the PEA with pitting and loss of bar area in several places. Pitting at the end extending towards the PEA.	Long splice bars performed well-some having stains at the splice location. Short splice bars exhibited the most corrosion of all beams. Many stains on epoxy coating and corrosion spread underneath the coating.	Stirrup in the middle was corroded. Pits were found underneath the epoxy coating. Of the two other stirrups at splice locations, one performed well while the other one had some damage, mostly around the corners.

PEA : Previously Exposed Area.

5.2 MACRO-CELLS

5.2.1 Half-Cell Potential Readings for Unencapsulated Macro-Cells

Figure 5.24 shows the results from the half-cell potential readings for the unencapsulated macro-cells. These readings were only taken for the control specimens since surface access was not possible for the encapsulated specimens. The readings indicate that the corrosion activity inside these macro-cells increased during the exposure cycles. This was confirmed later by visual observations.

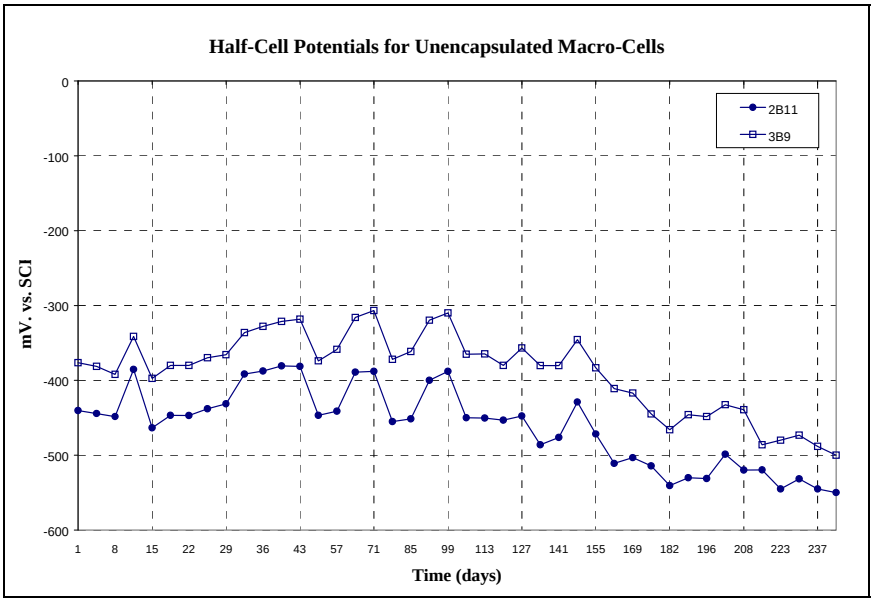

Figure 5.24. Half-Cell Potential reading for Unencapsulated Macro-Cells.

5.2.2 Macro-Cell Potential Readings

The macro-cell potentials throughout the duration of the encapsulation study as well as the previous study is shown in Figure 5.25 through 5.29. The previous study is shown as the TxDOT Program and the encapsulation study is shown as Encap. Program. There was a gap of 9 months between the two studies as shown. Analyzing the data, it is apparent that the polarity of the macro-cells changed during the study. Therefore, the readings are not very useful. The visual observations after opening the macro-cells confirm active corrosion in the black bars and indicate that the cathode and the anode were reversed. Since the macro-cells were designed to work in one direction (with the coated bars serving as the cathode), the change in polarity makes the readings meaningless. It was also noticed in the previous study that the readings became meaningless when the black bars started to corrode [Vaca, 1998].

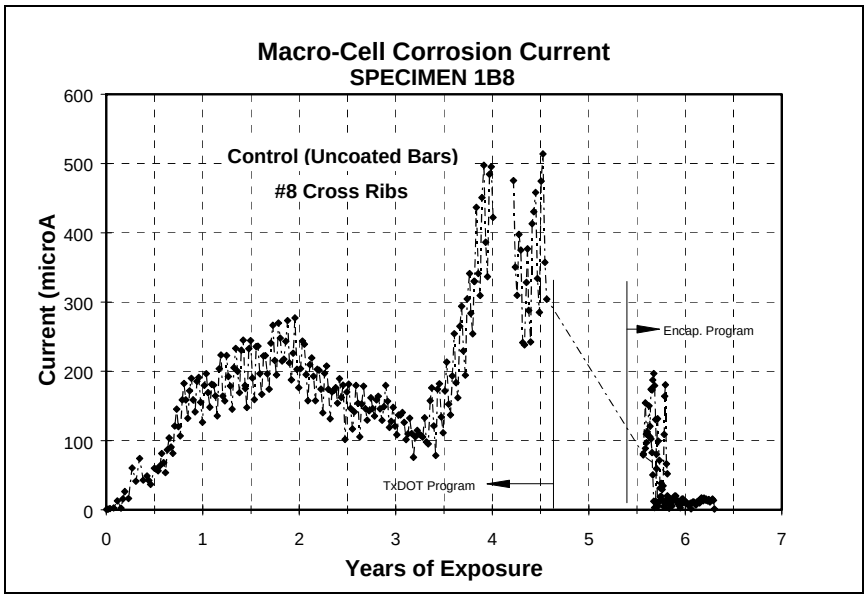

Figure 5.25. Macro-Cell Corrosion Current Readings for Specimen 1B8.

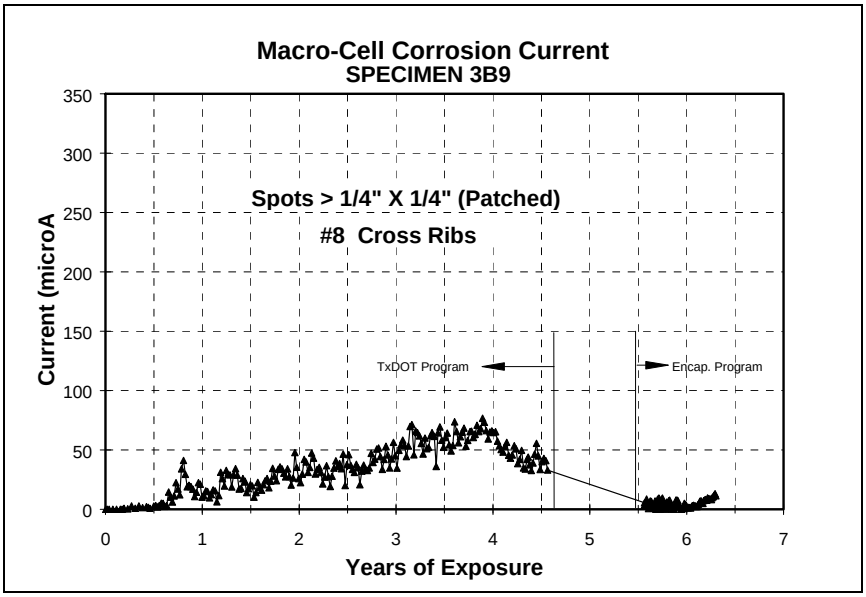

Figure 5.26. Macro-Cell Corrosion Current Readings for Specimen 3B9.

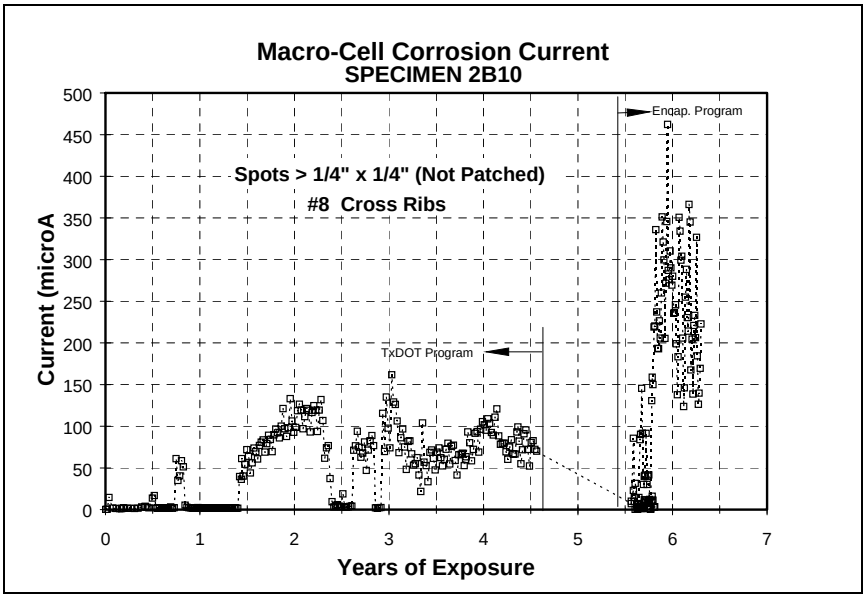

Figure 5.27. Macro-Cell Corrosion Current Readings for Specimen 2B10.

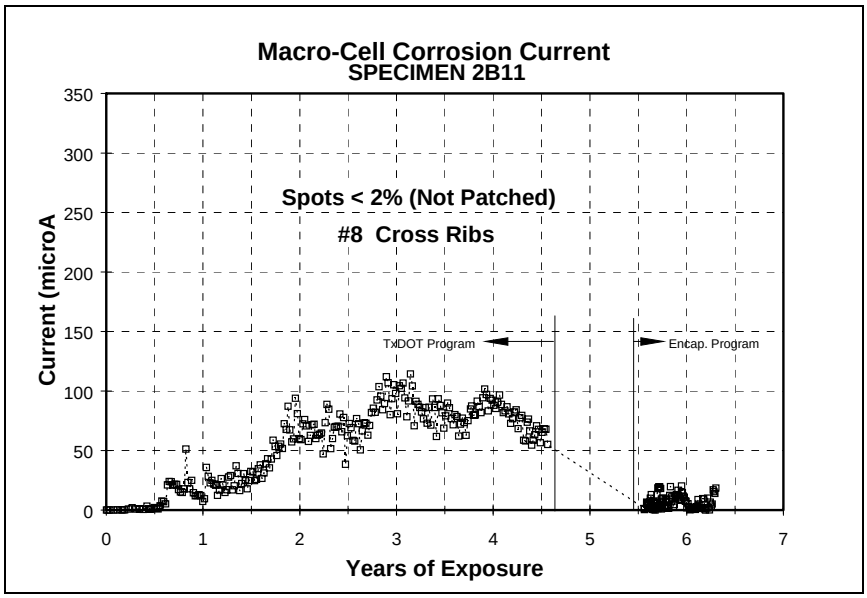

Figure 5.28. Macro-Cell Corrosion Current Readings for Specimen 2B11.

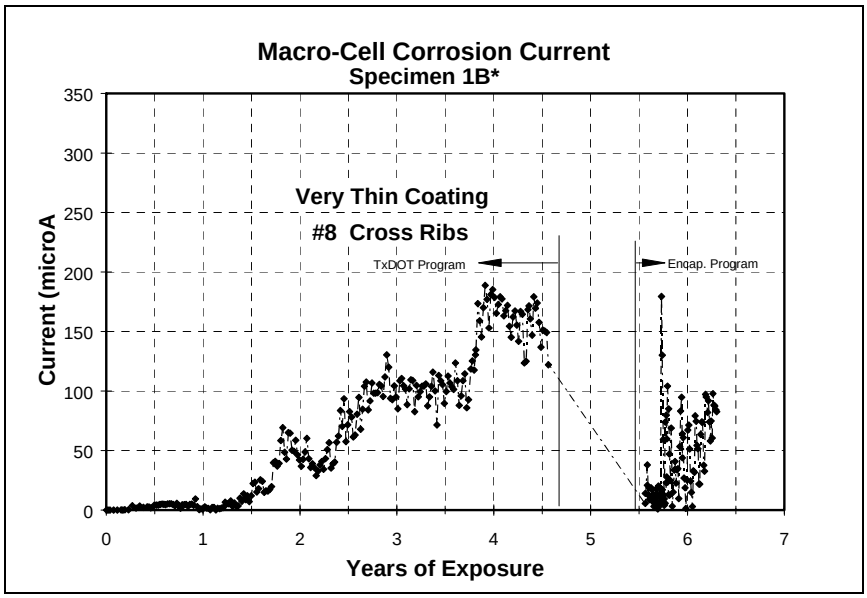

Figure 5.29. Macro-Cell Corrosion Current Readings for Specimen 1B*.

5.2.3 Chloride Content

Results from the chloride content analysis at the end of this study are compared with the results from the previous study in Table 5.3. It is seen that the chloride contents are lower than those from the previous study. Differences may be due to sampling errors.

Table 5.3. Summary of Chloride Content Testing for Macro-Cells.

		Avg. Chloride Content (%)	
Macro-Cell	**Avg. Depth (mm.)**	**Previous Study**	**This Study**
1B8	25-50	0.30	0.18
	75-100	0.20	0.11
1B*	25-50	0.36	0.21
	75-100	0.26	0.14
3B9	25-50	0.34	0.25
	75-100	0.20	0.12
2B10	25-50	0.34	0.14
	75-100	0.22	0.09
2B11	25-50	0.38	0.29
	75-100	0.30	0.10

5.2.4 Autopsies

When the macro-cells were opened, a green fluid was found in all the macro-cells on and near the straight black bars and on the bent black bar. 5.30, 5.31, and 5.32 show the fluid and stains on specimens 2B11, 3B9, and 2B10, respectively. Figure 5.33 shows the fluid staining the concrete after removing the bent black bar from specimen 1B8.

A lot of pitting damage was found both in black and in epoxy coated bent bars. Figures 5.34 and 5.35 show the pitting corrosion on the black bent bar and the severely stained concrete after this bar was removed. Similarly, Figures 5.36 and 5.37 show the pitting corrosion on epoxy coated bent bar and concrete stains after the bar was removed.

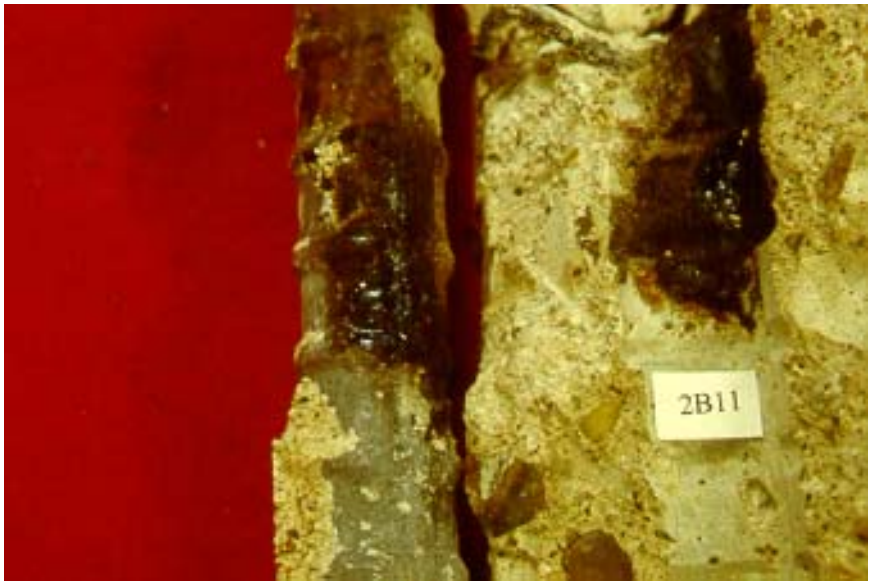

Figure 5.30. Corrosion Stains and Active Corrosion on Black Bars (2B11).

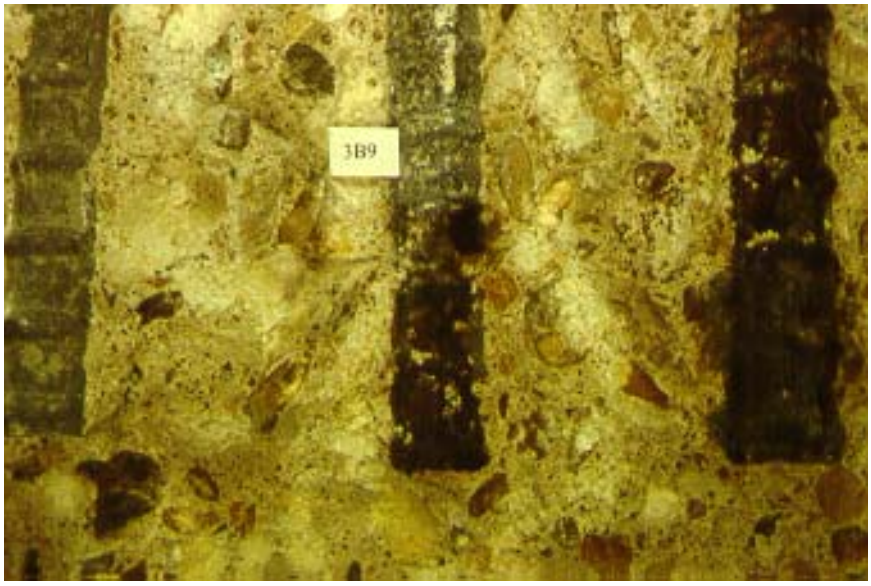

Figure 5.31. Corrosion Stains and Active Corrosion on Black Bars (3B9).

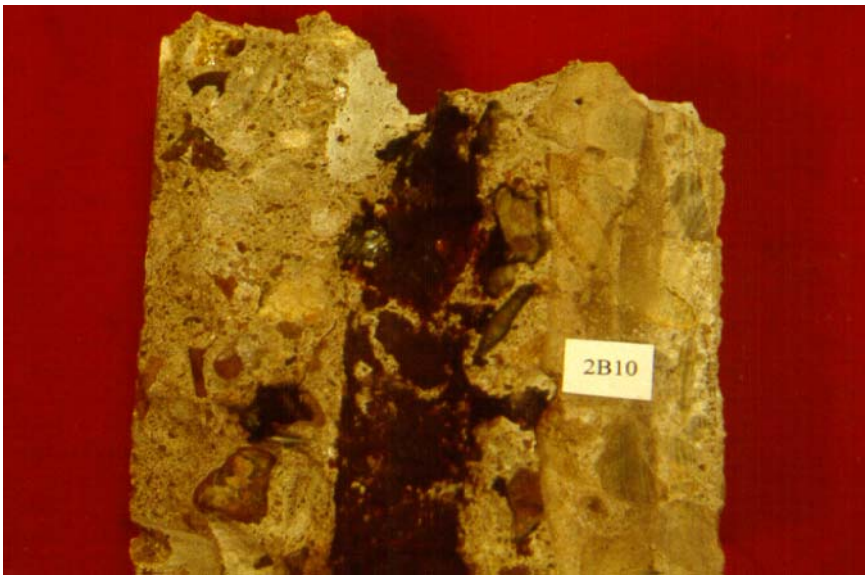

Figure 5.32. Corrosion Stains and Active Corrosion on Concrete (2B10).

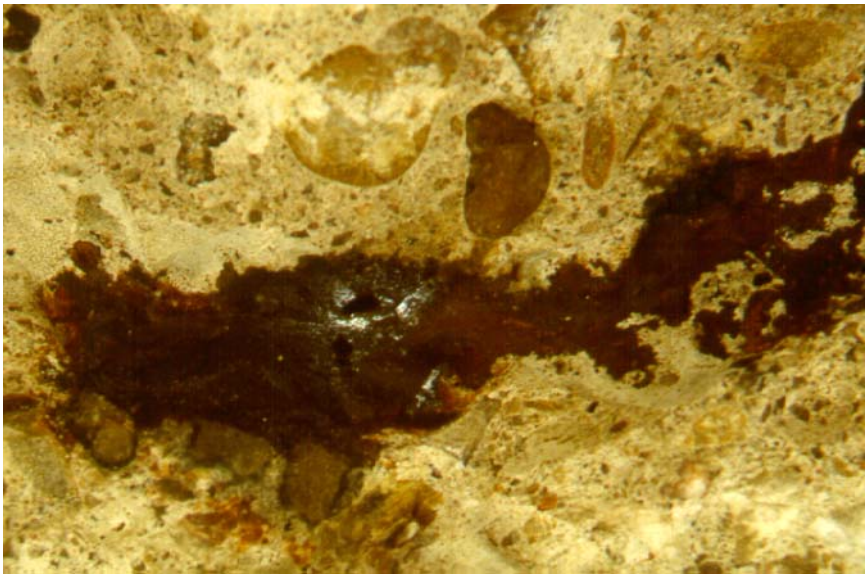

Figure 5.33. Active Corrosion on Concrete Bent Black Bar Side (1B8).

Figure 5.34. Damage on Bent Black Bar (1B8).

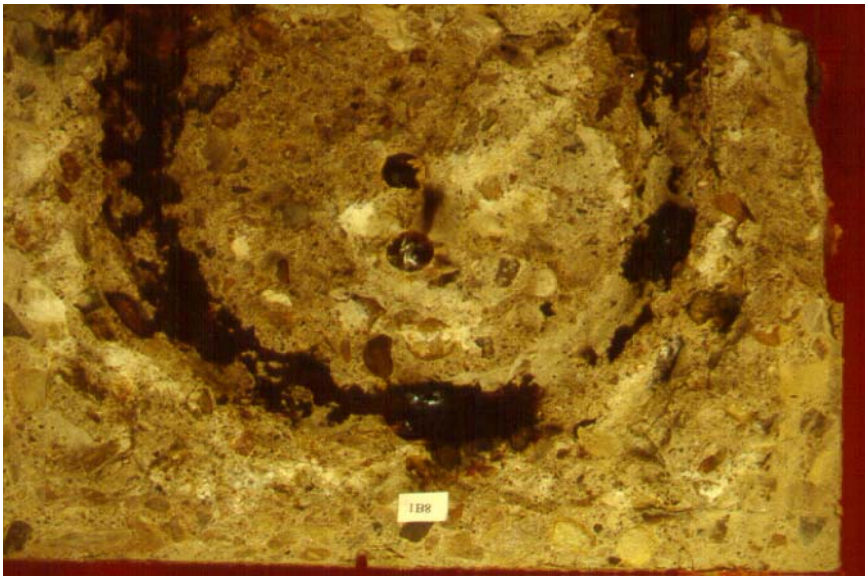

Figure 5.35. Damage on Concrete for Bent Black Bar (1B8).

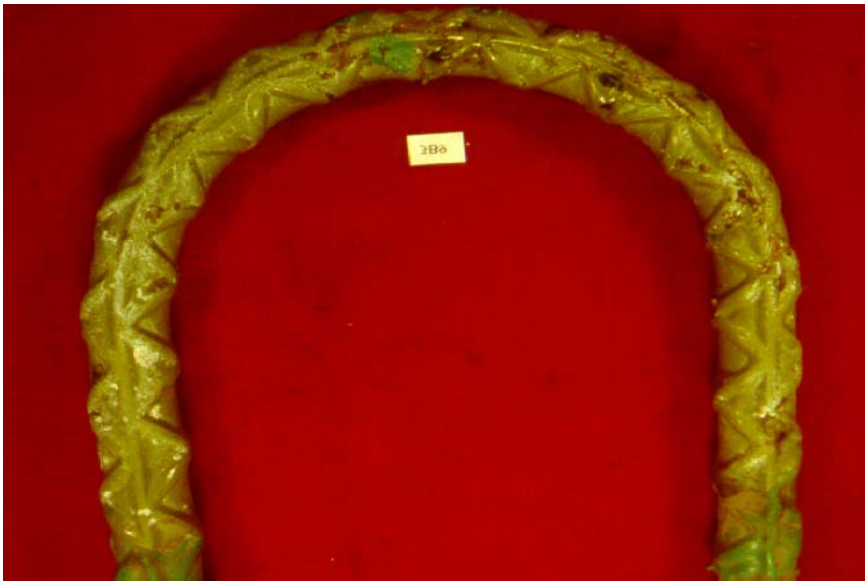

Figure 5.36. Pitting Damage on Epoxy Coated Bent Bar (3B9).

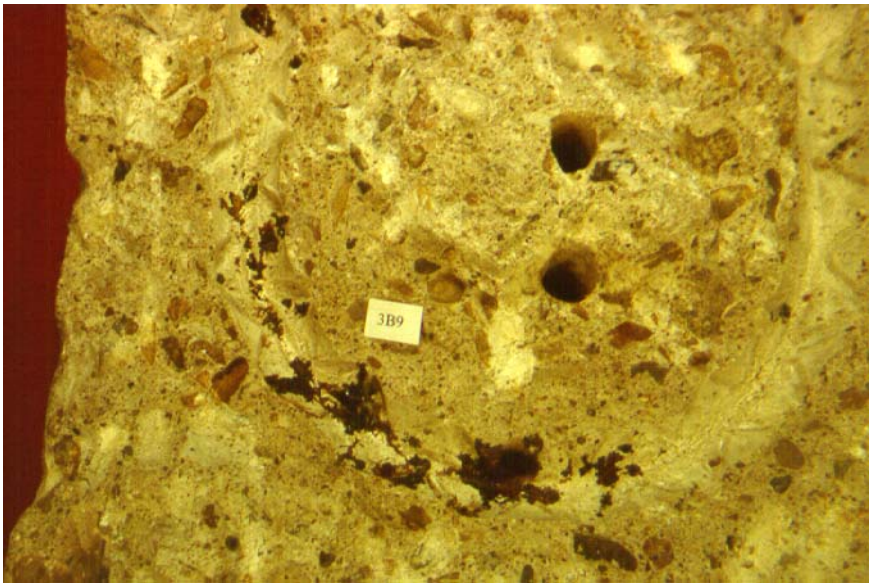

Figure 5.37. Damage on Concrete for Epoxy Coated Bar (3B9).

Figure 5.38 shows corrosion stains on a piece of concrete surface when the distribution media was peeled away. Corrosion may advance beneath the encapsulated surface but is not visible since the distribution media masks the stains. In field applications, encapsulation may eliminate the possibility of inspecting the surface for corrosion.

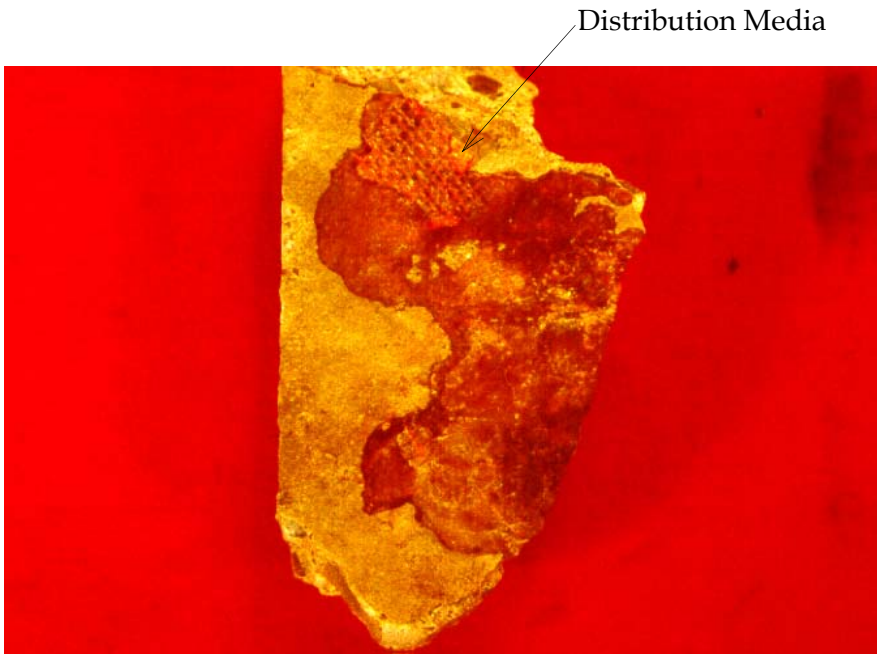

Figure 5.50. Corrosion Stains Underneath Epoxy and Distribution Media.

CHAPTER 6

SUMMARY AND CONCLUSIONS

6.1 SUMMARY

Corrosion of reinforcement in structural concrete is a major concern because of the economic impact of corrosion damage and the safety hazards that may result. Repair and rehabilitation of corrosion damaged structures is becoming increasingly important since the deterioration rate of existing structures increases with age. Therefore, research is being conducted in order to find new ways to protect against corrosion and new methods to repair corrosion damage in the most efficient way.

A new rehabilitation technique, encapsulation and epoxy injection (a procedure by Hardcore DuPont Composites) was tested in this study. Specimens which were exposed to a corrosive environment for four and a half years with well-documented corrosion data provided an ideal base for the program. Specimens repaired using encapsulation and epoxy injection were compared with specimens with no repair after a year of exposure to corrosive environment.

The specimens were monitored by taking half-cell potential readings throughout the duration of exposure. Additional acoustic emission testing was performed to investigate the applicability of this technique for corrosion

monitoring. At the end of the study the specimens were opened to examine the reinforcing bars inside the specimens.

6.2 CONCLUSIONS

From the experimental results obtained in this project, the following can be concluded:

The evacuation procedure did not remove moisture from the beams and there was no penetration of resin other than that at large cracks. Therefore, the beams were encapsulated with moisture trapped inside and encapsulating the concrete with moisture trapped inside may actually worsen the situation compared to a “bare” beam.

The encapsulation process eliminated the possibility of inspecting the concrete surface for signs of corrosion. Consequently, an encapsulated element can actually suffer severe corrosion without warning.

Epoxy coated bars performed well compared with uncoated bars and are recommended for field applications.

6.3 RECOMMENDATIONS FOR FURTHER RESEARCH

More research is needed in order to have a better understanding of the effect of encapsulation and epoxy injection for corrosion rehabilitation. Some issues to be studied are the removal of moisture from concrete, effectiveness of resin impregnation, and the corrosion process in an encapsulated element.

Active corrosion and corrosion in early stages was detected using acoustic emission and further research on use of acoustic emission methods for monitoring onset of corrosion is encouraged.

APPENDIX A

PROPERTIES OF HARDSHELL-CSRS PROCESS MATERIALS

Description: Product Data Sheet for the Hardshell Concrete Restoration System
Rev: A
Date: 12/5/96

1.0 System Description

1.1 Prefabricated E-glass shells are adhesively bonded to concrete structures to contain spalling, provide additional strength, extend life expectancy, and upgrade aesthetics. Thickness and orientation of shells is dependent on application. Entire system is coated with a methyl methacrylate coating.

2.0 Component Properties

2.1.0 The system components include: E-glass fabric, matrix resin, adhesive resin, and methyl methacrylate coating

2.1.1 E-glass fiber reinforcements

Typical aerial weights

0 Deg. Continuous Strand Roving	24.00 oz/yd^2	5.0% deviation
90 Deg. Continuous Strand Roving	16.00 oz/yd^2	5.0% deviation
+45 Deg. Continuous Strand Roving	12.00 oz/yd^2	5.0% deviation
- 45 Deg. Continuous Strand Roving	12.00 oz/yd^2	5.0% deviation
Mat	06.75 oz/yd^2	5.0% deviation
Stitch Yarns	00.05 oz/yd^2	5.0% deviation

2.1.2 Composite matrix resin (Derakane 411-350)

Typical clear cast properties

Tensile Strength	11000 psi.
Tensile Modulus	0.49 msi.
Compressive Strength	16000 psi.
Compressive Modulus	3.5 msi.
Elongation	5 %
Barcol Hardness	35

2.1.3 Adhesive Resin (Derakane 8084)

Typical mechanical properties

Property	**Test Method**	**Test Value (Tested at 77 deg. F)***
Lap Shear Strength (Fiberglass Composite Substrate)	ASTM D 1002	900 psi
Tensile Strength	ASTM D 638	10-11,000 psi.
Elongation	ASTM D 638	10-12 %
Heat Distortion temp	ASTM D 4065	170-180 deg. F
Barcol Hardness	ASTM D 2240	30

2.1.4 Methyl methacrylate coating (Eliminator S)

Typical mechanical properties

Property	Test Methods	Units
Water Vapor Transmission	ASTM 96-80	6.6 g/m^2/day
Adhesion to concrete	ASTM D4541	100psi
Adhesion to Steel	ASTM D4541	290 psi
Minimum Tensile Strength	ASTM D638	940 psi
Elongation	ASTM D638	80%

3.0 Laminate Information

3.1 All composite plates and angles are fabricated in a factory environment using the SCRIMP process (Seemann Composites Resin Infusion Molding Process). The SCRIMP process is a closed process that is highly reproducible. The vacuum driven process results in composites with low void and high fiber volume.

3.2 Fiberglass composite mechanical properties

Property at 72 deg. F	Test Method	Test Value
Tensile Modulus	ASTM D 3039	3.75 Msi.
Ultimate Tensile Strength	ASTM D 3039	70 ksi.
Strain	ASTM D 638	2.0 %
Fiber Volume Fraction	ASTM D 3171	54 %
Tg Composite Shells	ASTM D 4065	150 deg. F

4.0 Fiberglass adhesion information

4.1 All bonding surfaces are to be sandblasted for improved adhesion with the Derakane 8084. The sandblast must be uniform on the composite surface. The composite must be sandblasted with a fine grit sand until the fiberglass composite is feathered white.

4.2 Bond lines shall range from .03125" through .1875".

4.3 Minimum joint lap length for plate / angle lap joints is 4".

5.0 System installation requirements

5.1 The entire structure shall be covered with a minimum of a 40 mil methyl methacrylate coating.

5.2 No infusion shall be performed below 40 deg. F or above 100 deg. F.

5.3 No infusion shall be initiated until 27" Hg of vacuum is achieved and the system is left at said state for a minimum of 24 hours.

5.4 After infusion, vacuum (27" Hg) must remain on the system for a minimum of 16 hrs.

5.5 Acoustic or thermography verification shall be used to document void content.

5.6 Any voids greater than 1 sq ft shall require a secondary vacuum infusion.

5.7 Any voids ranging from .02 sq ft. through 1 sq ft shall require a secondary infusion. Pressure or vacuum assisted infusions are both acceptable.

5.8 All infusion ports shall be filled and coated with an epoxy or methyl methacrylate coating.

APPENDIX B

CORROSION DETECTION IN REINFORCED CONCRETE USING ACOUSTIC EMISSION AND ACOUSTIC EMISSION APPLICATION TO THE BEAMS

B.1 CORROSION DETECTION IN REINFORCED CONCRETE USING ACOUSTIC EMISSION

The corrosion process results in stress waves that can be picked up by acoustic emission sensors. These stress waves may be generated by either corrosion processes such as surface film growth and fracture, concrete matrix cracking, and cathodic bubble noise or by damage to the materials which might become emissive when subjected to stress such as area reduction, cracking, and pitting [Fowler, 1997; Pollock, 1986; Landis, 1994]. Also Weng et al. [1982], report that the acoustic emission from corroding and non-corroding specimens are different and that acoustic emission from corroding specimens is probably due to hydrogen gas evolution.

Research conducted at Northwestern University by Zdunek et all. show that early detection of steel rebar corrosion by acoustic emission is possible by using the steel as a waveguide. Researchers have also indicated that acoustic

emission can detect corrosion earlier than other traditional electric current measurements [Pollock, 1986; Landis, 1994; Zdunek, 1995].

B.2 ACOUSTIC EMISSION APPLICATION TO THE BEAMS

Acoustic emission testing of the beams was performed according to the Standard Procedure of Acoustic Emission Evaluation used by Association of American Railroads. The testing was performed using 60 kHz and 150 kHz sensors which were attached to bars protruding from the concrete. The steel was used as a waveguide to eliminate the attenuation problems encountered when sensors are attached to concrete.

Before the sensors were attached, the steel bars were ground to provide a smooth surface for attaching the sensors. The sensors were attached to the bars using high temperature hot melt glue. The sensors were then connected to a computer and evaluated. The standard procedure for acoustic emission evaluation was followed by breaking a pencil lead six inches apart from the face of the sensors in order to make sure that they were working properly and to characterize the attenuation. Pencil lead breaking was performed on the other bars inside the same beam and the sensor was still able to pick up the noise which meant that the corrosion on any bar can be detected by one sensor for each beam for this particular beam configuration. However, this might be different for field applications especially in large specimens due to attenuation.

After the system was checked, corrosion was monitored continuously for three days. The system was also monitored during the periodic loading and unloading of the beams which was carried out as part of the encapsulation study.

Figures B.1 and B.2 show the typical wave form for a hit obtained during the test. Figure B.3 shows the correlation plot after filtering the data obtained from the acoustic emission testing. The data obtained at the end of the acoustic emission testing program indicated that corrosion was occurring. The hits were short duration, medium amplitude (40-60 dB) and occurred in bursts of emission which are expected as indicated from previous corrosion tests in which acoustic emission was used.

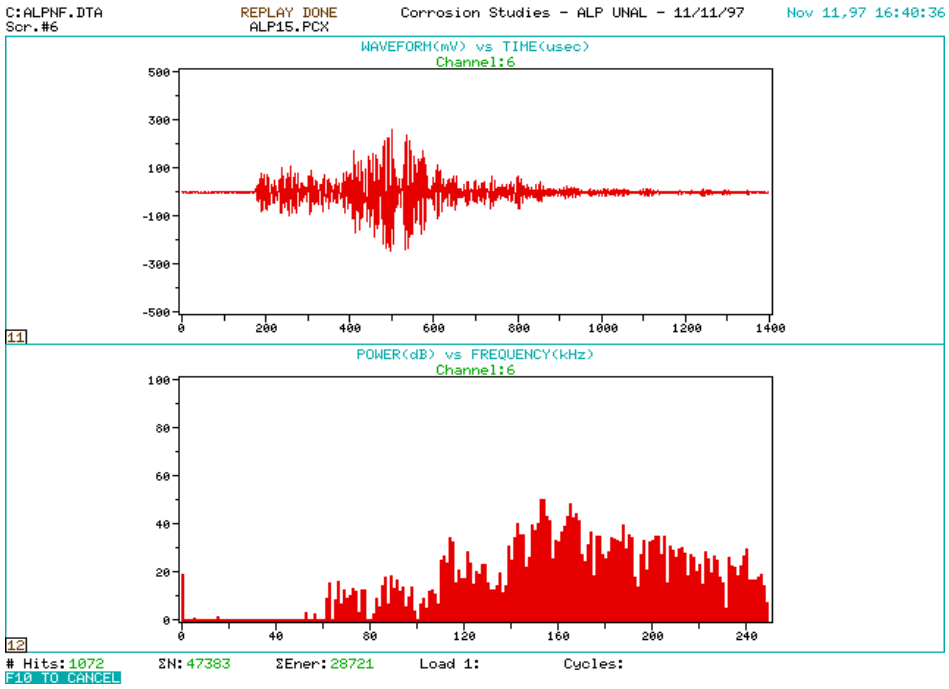

Figure B.1. Typical Wave Form.

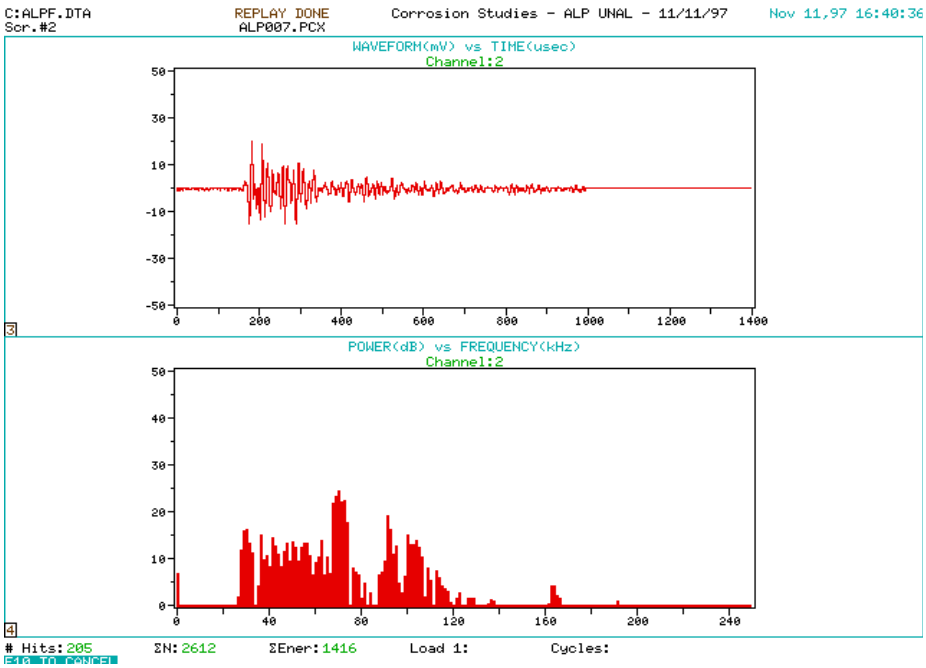

Figure B.2. Typical Wave Form.

Figures B.4 and B.5 show typical hits during loading of the beams. Figure B.6 is the correlation plot obtained during loading and loading of the beams. The hits were short duration and medium amplitude and the wave forms indicated occurrence of corrosion. The data shows the accelerated corrosion occurring during loading and unloading. After the loading and unloading process, the beams were quiet (no emission) for some time. The data was not produced by cracking or any damage to concrete due to loading since such damage generates emission of high amplitude (70-80 dB) and short duration.

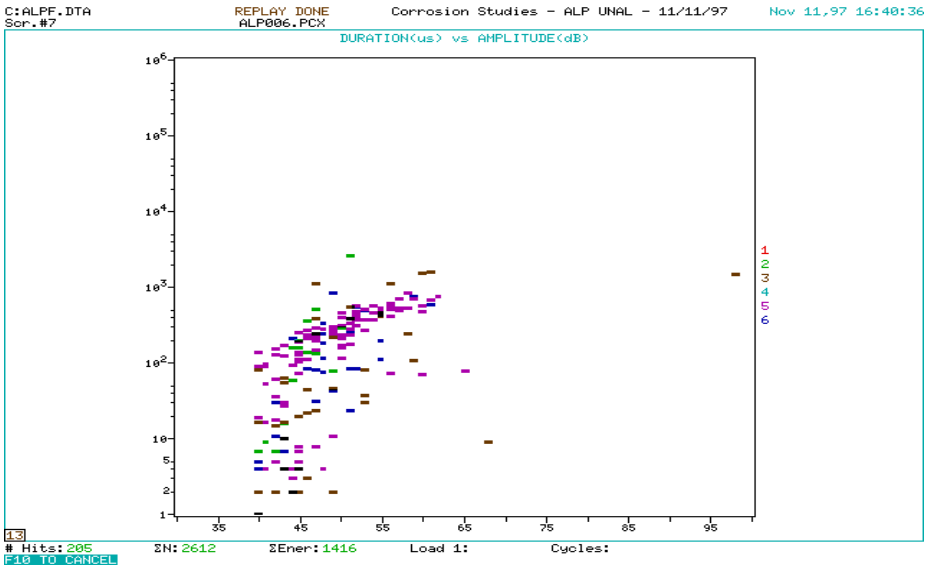

Figure B.3. Correlation Plot.

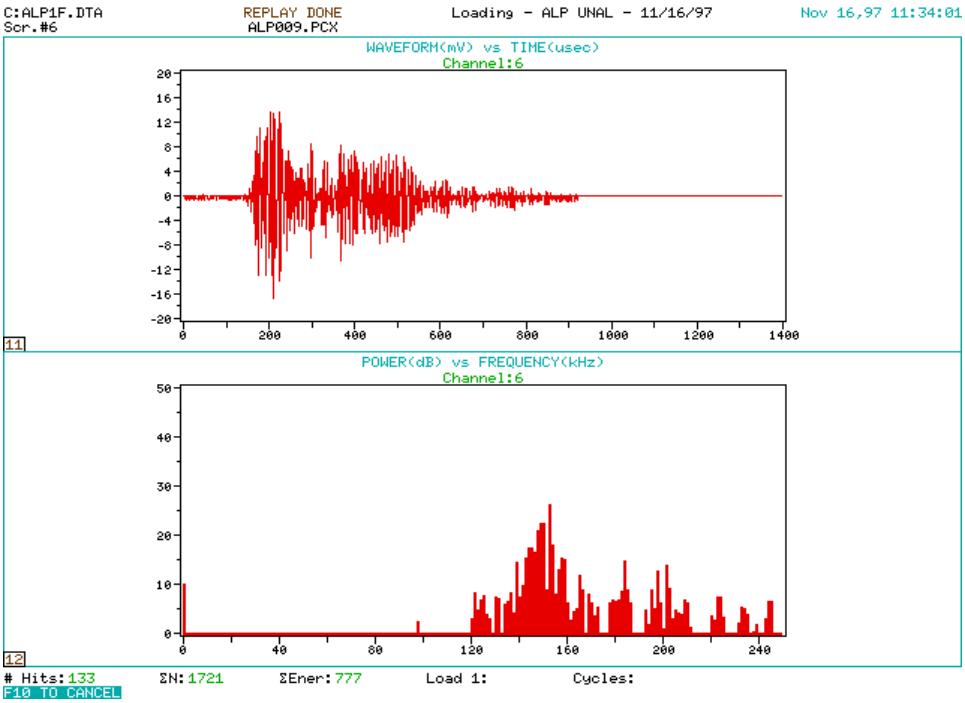

Figure B.4. Typical Wave Form During Loading.

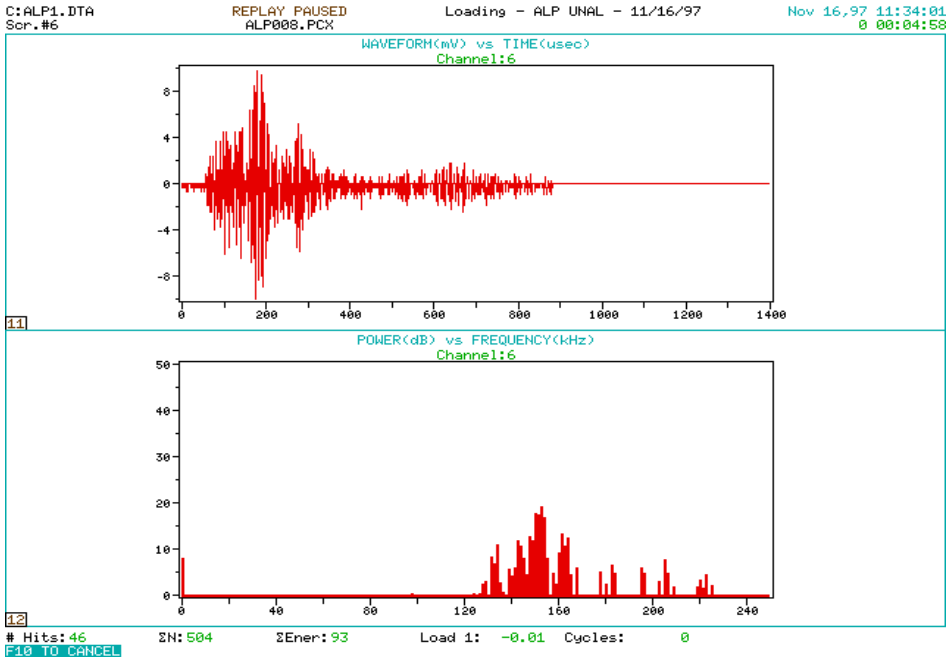

Figure B.5. Typical Wave Form During Loading.

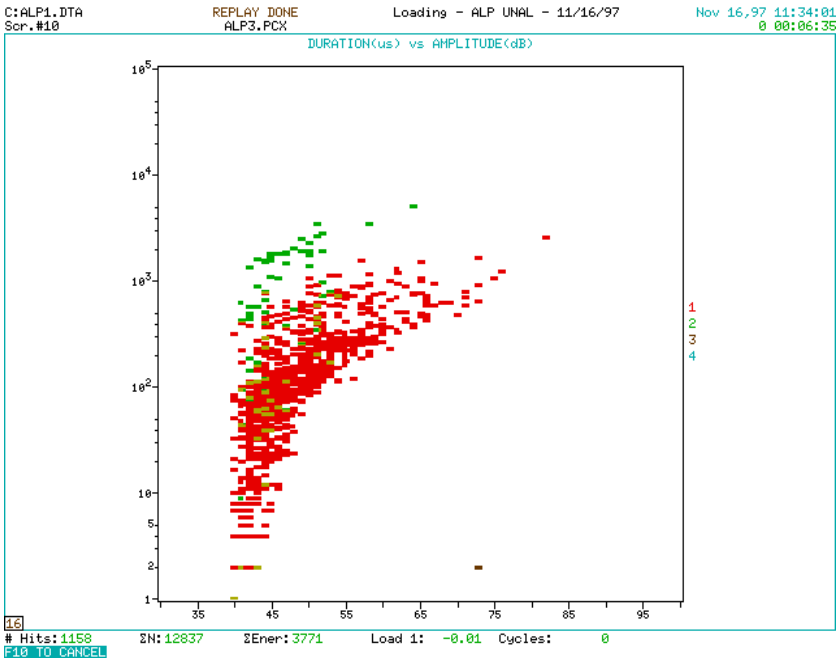

Figure B.6. Correlation Plot During Loading and Unloading.

The data obtained from the acoustic emission testing of beams show similarities with the research conducted at Northwestern University by Zdunek et all. which also utilized steel rebars as a waveguide [Landis, 1994; Zdunek, 1995]. When the wave forms in Figure B.1 are compared with the wave forms from the research conducted at the Northwestern University (Figure B.7), the similarity is obvious.

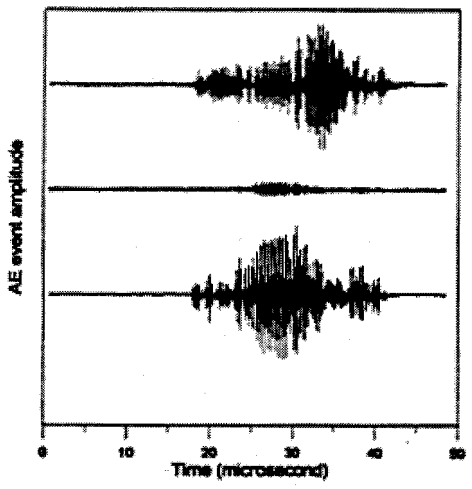

Figure B.7. AE Signal At Three Sensors for a Single AE Hit [Zdunek, 1995].

REFERENCES

Corrosion: Causes and Prevention, Speller, F. N., McGraw-Hill, New York, 1952.

Corrosion Engineering, Fontana, M. G., McGraw-Hill, New York, 1986.

Gibson, F. W. (Editor), "Steel Corrosion in Concrete: Causes and Restraints," ACI Publication SP-102, 1987.

Nene, R. L., "Repairs and Restoration of Reinforced Concrete Columns," ACI Publication SP-85-12, 1985, pp 260-263.

Gallegos, H., Quesada, G., "A Corrosion Case: Repair Procedure," Concrete International, June 1987, pp 54-57.

Pfeifer, D. W., "Steel Corrosion Damage on Vertical Concrete Surfaces- Part I. Causes of Corrosion and Useful Evaluation Tests," ACI Publication SCM-8, 1985, pp 117-119.

Pfeifer, D. W., "Steel Corrosion Damage on Vertical Concrete Surfaces- Part II. Causes of Corrosion and Useful Evaluation Tests," ACI Publication SCM-8, 1985, pp 120-124.

Maurisin, S. L., "Repairs of Concrete Columns, Spandrels, and Balconies on a High Rise Housing Complex in Chicago," ACI Publication SCM-8, 1985, pp 178-186.

Roberts, J. E. "Composite Construction in California Bridge Seismic Retrofitting," California Department of Transportation, Draft Special Provisions, 1997.

Fowler, T., "Class Notes," Austin, 1997.

Pollock, A. A., "Acoustic Emission Capabilities and Applications in Monitoring Corrosion," ASTM Publication STP-908, 1986.

Weng, M. S., et all., “Application of Acoustic Emission to Detection of Reinforcing Steel Corrosion in Concrete,” National Association of Corrosion Engineers, Vol. 38, No. 1, January, 1982.

Landis, E., et all., “Development of NDE of Concrete,” Northwestern University Center for Advanced Cement-Based Materials and BIRL Industrial Research Laboratory, June 1994.

Zdunek, A. D., et all., “Early Detection of Steel Rebar Corrosion by Acoustic Emission Monitoring,” National Association of Corrosion Engineers International Annual Conference and Corrosion Show 1995, Paper No. 547.

Kahhaleh, K. Z., “Corrosion Performance of Epoxy-Coated Reinforcement,” Ph.D. Dissertation, The University of Texas at Austin, May 1994.

Vaca, E., “Epoxy Coated Bars Corrosion ,” Ph.D. Dissertation, The University of Texas at Austin, May 1998.

American Society for Testing and Materials, “Half-Cell potentials of Uncaoted Reinforcing Steel in Concrete,” ASTM C876-87, Philadelphia, PA, 1987.-